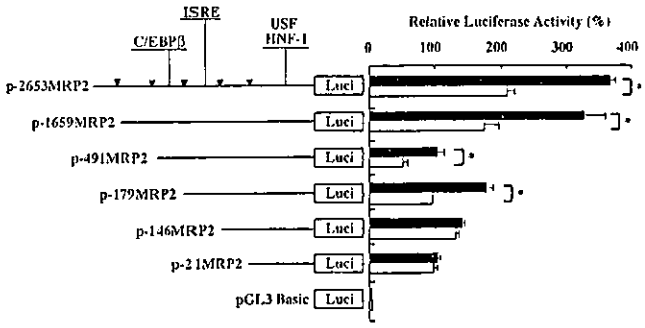

Fig. 4. Maps of the *MRP2* promoter luciferase constructs and the transcriptional activity of multidrug resistance protein 2 (MRP2) promoter-luciferase fusion plasmids transfected into HepG2 cells. Various lengths of human *MRP2* gene promoter plasmids containing the luciferase gene in the upstream region were constructed. Putative transcription factor binding sites on the *MRP2* promoter are also indicated. Luciferase activities were measured after 24 hours and were correlated for differences in transfection efficiency by *Renilla* luciferase activity, then normalized to the activity of the p-491 MRP2-Luci construct transfected into cells. Data are shown as the mean ± SD (**error bars**) of three independent experiments. $^*P < .01$. ISRE, interferon stimulatory response element; USF, upstream stimulatory factor; HNF-1, hepatic nuclear factor 1.

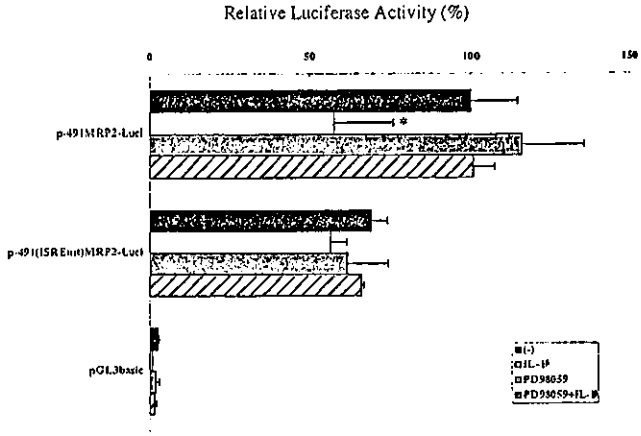

Fig. 6. Effects of PD98059 on interleukin-1β (IL-1β)-induced *MRP2* promoter suppression. p-491MRP2-Luci and p-491MRP2(ISREmt)-Luci were transfected into HepG2 cells. Six hours later, 20 μM PD98059 was administrated for 30 minutes and IL-1β was treated (20 ng/mL; 24 hours). This result was representative of three experiments. $^*P < .05$. MRP2, multidrug resistance protein 2; ISRE, interferon stimulatory response element.

moter. The construct designed contained a specific mutation in the consensus sequence of ISRE on the *MRP2* promoter (AGAAGCGAAACT to AcgtGCGcgtCT). To check the adjacent transcription factors, we also made C/EBPβ, HNF 1, and USF mutant constructs (Fig. 5). We transfected the mutant p-491MRP2-Luci constructs into HepG2 cells in the absence or presence of IL-1β. Compared with the wild-type construct, the ISRE mutant reporter gene constructs showed a slightly lower basal activity in comparison with the wild type. Introduction of mutation into USF (USFmt) did not affect the basal promoter activity, whereas the HNFmt construct showed a marked decrease in the basal promoter activity, suggesting that HNF plays a key role in the *MRP2* basal promoter activity. C/EBPmt construct enhanced the basal promoter activity by approximately 170% compared with the wild-type construct, indicating a negative regulatory role of C/EBPβ. When the p-491 MRP2 ISREmt was treated with IL-1β, no suppression of reporter gene activity was observed. There was a significant decrease in the promoter activity of IL-1β-treated USFmt, HNFmt, and C/EBPβmt reporter constructs (Fig. 5). These results indicated that the ISRE element specifically contributes to both basal promoter activity and IL-1β responsive down-regulation in *MRP2* promoter constructs.

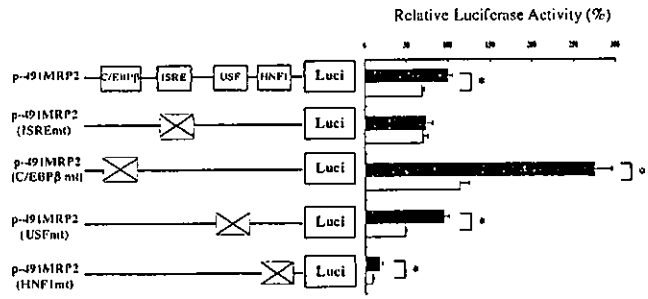

Fig. 5. Transcriptional activity of p-491 MRP2-Luci and 4 p-491 MRP2 mutant-Luci (interferon stimulatory response element [ISRE], C/EBPβ, hepatic nuclear factor 1 [HNF1], and upstream stimulatory factor [USF]) transfected into HepG2 cells with or without 20 ng/mL of interleukin-1β (IL-1β) for 24 hours. Various mutant forms of human *MRP2* gene promoter plasmids containing the luciferase gene in the upstream region were constructed. Luciferase activities were measured after 24 hours and were corrected for differences in transfection efficiency by *Renilla* luciferase activity, then normalized to the activity of the p-491 MRP2-Luci construct transfected into cells. This result was representative of three experiments. $^*P < .01$. MRP2, multidrug resistance protein 2.

To investigate whether an ERK inhibitor, PD98059, affects IL-1β-mediated suppression of *MRP2* promoter activity, we performed a transient transfection assay with p-491 MRP2-Luci and p-491(ISREmt) MRP2-Luci constructs in the presence or absence of this drug (Fig. 6). IL-1β again reduced the promoter activity of p-491 MRP2, and pretreatment with PD98059 significantly reduced IL-1β-mediated suppression of *MRP2* promoter activity. The basal promoter activity of p-491 (ISREmt) MRP2 was decreased relative to that of p-491 MRP2, and the suppression of the promoter activity of the mutant construct by IL-1β was not significant (Fig. 6). Coadministration of PD98059 seemed to have no effect on the p-491MRP2 (ISREmt)-driven luciferase activity.

Binding of IRF3 to ISRE on MRP2 Promoter is Reduced by IL-1β. EMSAs were performed to investigate the binding of IRF3 to *MRP2* promoter ISRE ele-

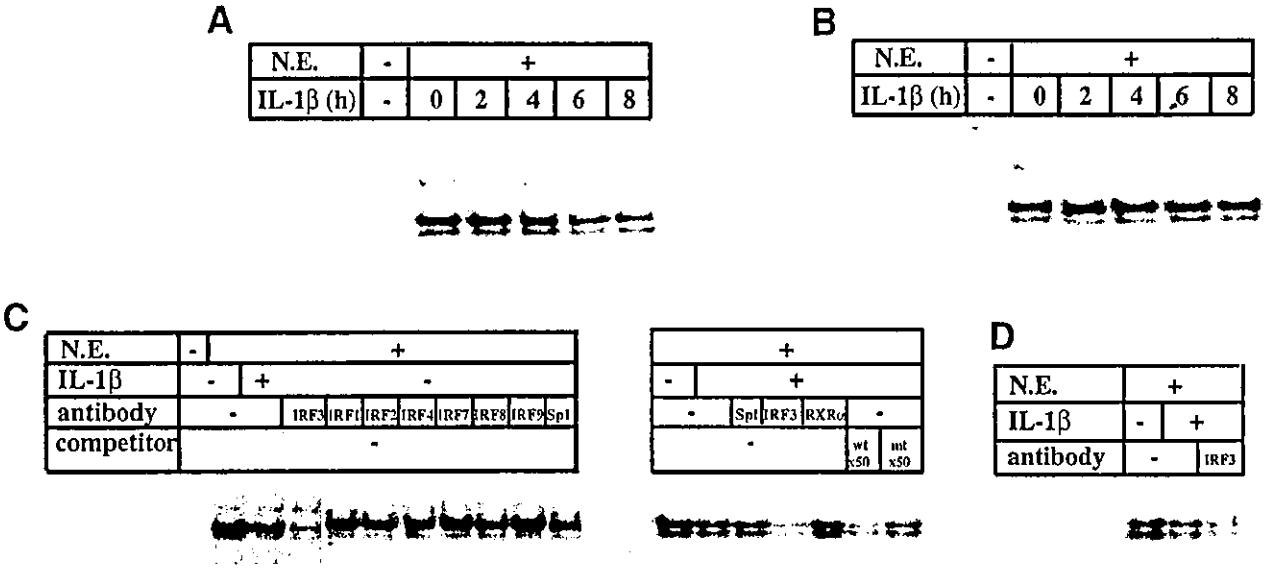

Fig. 7. Binding of IRF3 to *MRP2* promoter interferon stimulatory response elements (ISREs). Electrophoretic mobility shift assay (EMSA) was performed using radiolabeled probes, including interferon stimulatory response element (ISRE; −171/−159, 5′-GCAGCAGAAGCGAAACTGCAC-3′). For the competition assay, the unlabeled ISRE mutant probe (−179/−153: 5′-GCAGCAcgtGCGcgtCTGCA-3′) was used as a competitor. (A) Effects of interleukin-1β (IL-1β) on nuclear protein-ISRE binding. Cells were incubated with 20 ng/mL IL-1β for 0 to 8 hours. The nuclear extracts were prepared, and the extracts (4 μg of protein) that were incubated with ^{32}P-labeled oligonucleotide were resolved by gel electrophoresis. (B) Effects of PD98059 on IL-1β-induced *MRP2* downregulation. Before IL-1β stimulation, 20 μM PD98059 was administrated for 30 minutes. (C) Super shift and competition assay using nuclear extract with or without IL-1β for 8 hours. Anti-IRF1-4, 7-9, Sp1, and RXRα antibodies were added to the nuclear extracts. A 50-fold excess of the unlabeled oligonucleotide was added for the competition. (D) EMSA using nuclear extract from normal human hepatocytes (hNHeps). A bracket ([) indicates the DNA protein complex. These results were representative of three experiments. IRF, interferon regulatory factor; RXR, retinoid X receptor; MRP2, multidrug resistance protein 2.

ments in nuclear extract from HepG2 cells. EMSA using radiolabeled ISRE oligonucleotides and nuclear extract showed two bands corresponding to specifically bound complexes (Fig. 7A). These ISRE–protein complex bands were reduced by treatment with 20 ng/mL IL-1β for 6 to 8 hours in the absence of an ERK inhibitor (Fig. 7A). By contrast, no decrease of ISRE–protein complex formation was observed when PD98059 was coadministered with IL-1β (Fig. 7B).

We next examined whether these diminished bands represented specific binding to ISRE and attempted to determine which protein was involved in the ISRE–protein complex formation. We used cold competitors and specific antibodies for IRF family members (Fig. 7C). A 50-fold excess of ISRE wild-type cold competitor was sufficient to abolish these bands. However, the retarded bands were not abolished when treated with mutant competitors (Fig. 7C), suggesting that the bands represented specific binding to the ISRE element. All members of the IRF family share homology in the DNA binding domain and bind to a similar DNA motif, the ISRE.[24,25] We performed supershift assays using antibodies of IRF family proteins IRF1, IRF2, IRF3, IRF4, IRF7, IRF8, and IRF9. As shown in Fig. 7C, the retarded bands were abolished specifically only when treated with anti-IRF3 antibody. Other IRF antibodies, Sp1 and RXR, retinoid X receptor (RXR) antibody, failed to shift these bands (Fig. 7C). This suggested that these two bands contain IRF3 protein–DNA complexes. IRF3 thus seemed to bind specifically to the ISRE element of the MRP2 promoter, and IRF3 binding activity to ISRE seemed to be reduced by treatment with IL-1β. We next examined whether nuclear extract from human primary hepatocytes instead of HepG2 could bind to ISRE elements. We observed that the specific ISRE–protein complex bands from human primary hepatocyte were reduced by treatment with IL-1β (Fig. 7D). We also observed that these retarded bands were abolished specifically when pretreated with anti-IRF3 antibody. These results suggested that human primary hepatocytes contain the IRF3 protein–DNA complexes.

Decreased IRF3 Translocation Into the Nucleus on Treatment With IL-1β. The reduction in IRF3 binding to ISRE could account for the observed IL-1β-mediated downregulation of *MRP2* mRNA expression. Reduced binding to ISRE could be caused by a lower expression of IRF3 at the protein level, or by the modification of IRF3 affecting DNA binding or nuclear import. We therefore investigated the expression of IRF3 after IL-1β treatment in the entire cell fraction (Fig. 8A, left), nuclear fraction

(Fig. 8A, middle), and cytoplasmic fraction of HepG2 cells (Fig. 8A, right). IRF3 is a phosphoprotein that is constitutively expressed in two forms of approximately 55 kD[26] in unstimulated HepG2 cells (Fig. 8A). The upper band of IRF3 could be basal IRF3 phosphorylation corresponding to the N-terminal of IRF3. In the nucleus, IRF3 protein abundance was reduced in this compartment when cells were treated with IL-1β for 8 hours. No reduction in cytoplasmic IRF3 protein and no change in the level of phosphorylation was observed when treated with IL-1β. High mobility group protein-I and glucose-6-phosphate dehydrogenase were used as markers for nuclear and cytoplasmic fraction, respectively. Pretreatment with PD98059 almost completely abolished the IL-1β-induced reduction of nuclear IRF3 protein level, even when cells were treated with IL-1β for 8 hours (Fig. 8B). IL-1β treatment did not change IRF3 protein levels in the whole cell fraction (Fig. 8A,B). To investigate the potential action of IRF3 on *MRP2* promoter activity, we used IRF3 expression vector fused Flag tags. The Flag-IRF3 or Flag-only vector was transiently cotransfected into HepG2 cells with a MRP2 promoter luciferase construct for 48 hours. Introduction of Flag-IRF3 from 20 to 200 ng induced an approximately 1.5- to 2.0-fold increase in wild-type *MRP2* promoter activity (Fig. 9). By contrast, no induction by Flag-IRF3 was observed when the ISRE mutant reporter was assayed. These results suggested that IRF3 may be involved in the basal transcriptional activity of the *MRP2* promoter through the ISRE element.

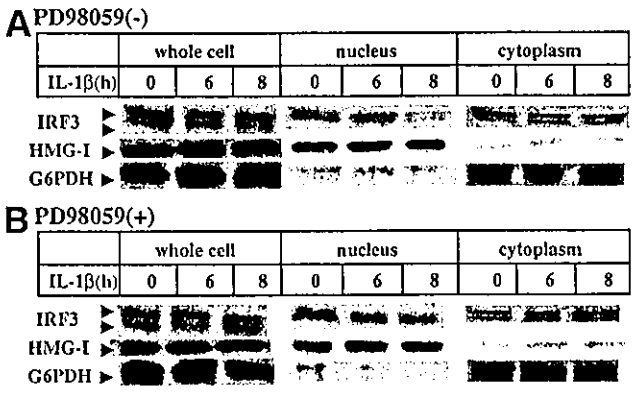

Fig. 8. Alteration of interferon regulatory factor 3 (IRF3) protein levels in HepG2 in response to interleukin-1β (IL-1β) administration with or without PD98059. 50 μg of whole cell lysate (**left panel**), 30 μg of nuclear extracts (**center**), and 50 μg of cytoplasmic extracts (**right**) were loaded onto each lane. (B) 20 μM PD98059 was administrated for 30 minutes before IL-1β stimulation. Anti-HMG-I antibodies and anti-glucose-6-phosphate dehydrogenase antibodies were used as nuclear and cytoplasmic protein controls. This result was representative of three experiments. HMG-I, high mobility group protein I.

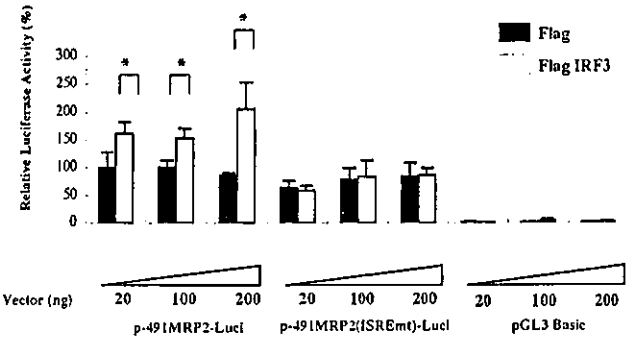

Fig. 9. Alteration of *MRP2* promoter-luciferase activity by expression of rIRF3 in HepG2 cells. Cells were transiently transfected with each construct, pRL-TK, and Flag or Flag-IRF3 for 24 hours and assayed for luciferase activity. Luciferase activities were corrected for differences in transfection efficiency by *Renilla* luciferase activity and were normalized to the activity of the pGL3 basic vector transfected into cells. Each dose of Flag or Flag-IRF3 was transiently transfected. This result was representative of three experiments. $^*P < .01$. IRF3, interferon regulatory factor 3.

Discussion

Cholestasis and hyperbilirubinemia are common clinical features in various hepatic diseases, including virus-induced or drug-induced hepatitis, alcoholic hepatitis, sepsis, and idiopathic postoperative cholestasis.[27,28] Endotoxins and proinflammatory cytokines are thought to be among the main mediators of inflammation-induced cholestasis.[29,30] Recent studies have reported on the manner by which bile salts or cholesterol homeostasis-regulatory mechanisms are controlled through enterohepatic circulation at the molecular level. Altered expression levels of various transporters, including ABC transporters, have been implicated in cholestasis.[31] MRP2 is a typical canalicular ABC transporter that exports many essential organic anions. We previously characterized the 5′-flanking region of the human *MRP2* gene and its promoter activity in human hepatic cells.[4,20] Our subsequent study[19] demonstrated that *MRP2* promoter (p-2635)-driven luciferase activity in hepatic cells was greatly inhibited by IL-1β, and less so by TNFα or IL-6. Consistent with this study, our present study also indicates that *MRP2* promoter activity is highly susceptible to the inflammatory cytokine IL-1β. In this study, we demonstrate that treatment of HepG2 cells with IL-1β results in decreased levels of *MRP2* mRNA transcription. In addition, we demonstrate that a regulatory protein, IRF3, is responsible for the IL-1β-induced downregulation of *MRP2*. IRF3 activates the *MRP2* promoter through the ISRE under unstimulated conditions. Treatment with IL-1β induces a decrease in both nuclear accumulation of IRF3 and IRF3 binding to ISRE, resulting in downregulation of the *MRP2* gene.

Other incidences of IL-1β inducing downregulation of transporters have been reported recently. Denson et al.[32] reported that rat *ntcp* and *mrp2* genes are regulated by retinoic acid receptor:RXR, and that IL-1β reduces nuclear retinoic acid receptor:RXR. The retinoic acid receptor:RXR site is located in −210/−180 bp upstream from the transcription initiation site in the human *MRP2* promoter.

Our promoter deletion analysis and mutation of the promoter show that the IL-1β-induced inhibition of *MRP2* promoter activity is the result of the ISRE region downstream of retinoic acid receptor:RXR. It has also been reported that IL-1β-induced downregulation of the rat *ntcp* gene occurs via the JNK pathway,[33] whereas in our study, the downregulation of human *MRP2* by IL-1β occurs via the ERK pathway. Kast et al.[34] also reported that rat *mrp2* expression is regulated by the pregnane X receptor and constitutive androgen receptor, and that rat *mrp2* promoter activity is activated by nuclear receptor pregnane X receptor, constitutive androgen receptor, and their agonist. These results suggest that *MRP2* expression in the liver is regulated by environmental stimuli, numerous compounds through various nuclear receptors, and IRF3. The 5′-flanking region of the *MRP2* promoter contains C/EBPβ, HNF1, and USF elements, as well as an ISRE (Fig. 5).[20] Mutant constructs of ISRE and HNF show decreasing basal promoter activities when compared with the wild-type *MRP2* promoter, suggesting that these elements play a key role in the basal promoter activity. By contrast, there is an almost 3.0-fold increase in the promoter activity by a C/EBPβ mutation in the context of the *MRP2* promoter over wild type. Thus, C/EBPβ may regulate *MRP2* promoter activity negatively. We observed that IL-1β-induced suppression of *MRP2* mRNA is associated with the ISRE region of the *MRP2* promoter (Fig. 5). Among the various factors interacting with ISRE, IRF3 was found to bind specifically to the ISRE on the *MRP2* promoter (Fig. 7). EMSAs show two bands containing IRF3–protein complexes. These complexes may be the result of different proteins interacting with IRF3 or conformational changes within the protein. Expression of the exogenous IRF3 gene increases MRP2 promoter activity through the ISRE and when cells are treated with IL-1β levels of IRF3 in the nucleus are diminished (Fig. 8). IRF3 thus seems to be a positive transcription factor of the *MRP2* promoter in hepatic cells, and decreased levels of IRF3 in the nucleus may be responsible for IL-1β-induced downregulation of the *MRP2* promoter activity. However, we could not ruled out other transcription factor in IL-1β-mediated suppression of MRP2.

Infection of fibroblasts with human cytomegalovirus also causes nuclear translocation of IRF3 and cooperative DNA binding with the transcriptional coactivator CBP/p300.[35] On infection of a cell with a virus, the C-terminal domain of cytoplasmic IRF3 is phosphorylated and translocated to the nucleus of hematopoietic cells, where it activates several virus-induced genes.[26] Our work shows that IRF3 is expressed continuously in both the nucleus and cytoplasm of hepatic cells (Fig. 8). Uchiumi et al. (unpublished data). have demonstrated by immunohistochemical study that IRF3 is found to be localized mainly to the cytoplasm, with 10% of whole cell IRF3 in the nucleus. We observe a marked decrease in IRF3 protein levels in the nucleus accompanied by reduced formation of the IRF3–DNA complex when cells are treated with IL-1β for 6 hours or longer.

Coadministration of an ERK inhibitor (PD98059) relieves the suppression of *MRP2* mRNA expression and *MRP2* promoter activation by IL-1β and reverses the decreased binding of IRF3 to ISRE seen in the presence of IL-1β. IL-1β seems to decrease nuclear levels of a positive regulatory factor, IRF3, resulting in suppression of the *MRP2* promoter through the loss of interaction with ISRE. This process of IL-1β-induced suppression of the *MRP2* gene could be linked closely with ERK1/2 activation signaling.

In conclusion, among the many interferon regulatory factors, we determined that IRF3 has a specific interaction with ISRE on the *MRP2* promoter. The expression of exogenous IRF3 in hepatic cells activates reporter gene expression via the p-491MRP2 promoter construct containing wild-type ISRE, but not by p-491MRP2 (ISREmt) containing mutant ISRE. The expression levels of IRF3 in the nucleus decrease after cells are treated with IL-1β for 8 hours, concomitant with a reduction in the binding of IRF3 to ISRE at the MRP2 promoter.

References

1. Oude Elferink RP, Groen AK. The role of mdr2 P-glycoprotein in biliary lipid secretion. Cross-talk between cancer research and biliary physiology. J Hepatol 1995;23:617–625.
2. Elferink RO, Groen AK. Genetic defects in hepatobiliary transport. Biochim Biophys Acta 2002;1586:129–145.
3. Kuwano M, Uchiumi T, Hayakawa H, Ono M, Wada M, Izumi H, et al. The basic and clinical implications of ABC transporters, Y-box-binding protein-1 (YB-1) and angiogenesis-related factors in human malignancies. Cancer Sci 2003;94:9–14.
4. Taniguchi K, Wada M, Kohno K, Nakamura T, Kawabe T, Kawakami M, et al. A human canalicular multispecific organic anion transporter (cMOAT) gene is overexpressed in cisplatin-resistant human cancer cell lines with decreased drug accumulation. Cancer Res 1996;56:4124–4129.
5. Paulusma CC, Bosma PJ, Zaman GJ, Bakker CT, Otter M, Scheffer GL, et al. Congenital jaundice in rats with a mutation in a multidrug resistance-associated protein gene. Science 1996;271:1126–1128.
6. Suzuki H, Sugiyama Y. Single nucleotide polymorphisms in multidrug resistance associated protein 2 (MRP2/ABCC2): its impact on drug disposition. Adv Drug Deliv Rev 2002;54:1311–1331.

7. Paulusma CC, Kool M, Bosma PJ, Scheffer GL, ter Borg F, Scheper RJ, et al. A mutation in the human canalicular multispecific organic anion transporter gene causes the Dubin-Johnson syndrome. HEPATOLOGY 1997;25: 1539–1542.
8. Toh S, Wada M, Uchiumi T, Inokuchi A, Makino Y, Horie Y, et al. Genomic structure of the canalicular multispecific organic anion-transporter gene (MRP2/cMOAT) and mutations in the ATP-binding-cassette region in Dubin-Johnson syndrome. Am J Hum Genet 1999;64:739–746.
9. Wada M, Toh S, Taniguchi K, Nakamura T, Uchiumi T, Kohno K, et al. Mutations in the canilicular multispecific organic anion transporter (cMOAT) gene, a novel ABC transporter, in patients with hyperbilirubinemia II/Dubin-Johnson syndrome. Hum Mol Genet 1998;7:203–207.
10. Thorgeirsson SS, Huber BE, Sorrell S, Fojo A, Pastan I, Gottesman MM. Expression of the multidrug-resistant gene in hepatocarcinogenesis and regenerating rat liver. Science 1987;236:1120–1122.
11. Trauner M, Arrese M, Soroka CJ, Ananthanarayanan M, Koeppel TA, Schlosser SF, et al. The rat canalicular conjugate export pump (Mrp2) is down-regulated in intrahepatic and obstructive cholestasis. Gastroenterology 1997;113:255–264.
12. Vos TA, Hooiveld GJ, Koning H, Childs S, Meijer DK, Moshage H, et al. Up-regulation of the multidrug resistance genes, Mrp1 and Mdr1b, and down-regulation of the organic anion transporter, Mrp2, and the bile salt transporter, Spgp, in endotoxemic rat liver. HEPATOLOGY 1998;28:1637–1644.
13. Vos TA, Van Goor H, Tuyt L, De Jager-Krikken A, Leuvenink R, Kuipers F, et al. Expression of inducible nitric oxide synthase in endotoxemic rat hepatocytes is dependent on the cellular glutathione status. HEPATOLOGY 1999;29:421–426.
14. Gerloff T, Geier A, Stieger B, Hagenbuch B, Meier PJ, Matern S, et al. Differential expression of basolateral and canalicular organic anion transporters during regeneration of rat liver. Gastroenterology 1999;117:1408–1415.
15. Hartmann G, Cheung AK, Piquette-Miller M. Inflammatory cytokines, but not bile acids, regulate expression of murine hepatic anion transporters in endotoxemia. J Pharmacol Exp Ther 2002;303:273–281.
16. Genin P, Algarte M, Roof P, Lin R, Hiscott J. Regulation of RANTES chemokine gene expression requires cooperativity between NF-kappa B and IFN-regulatory factor transcription factors. J Immunol 2000;164: 5352–5361.
17. Barnes B, Lubyova B, Pitha PM. On the role of IRF in host defense. J Interferon Cytokine Res 2002;22:59–71.
18. Hiscott J, Pitha P, Genin P, Nguyen H, Heylbroeck C, Mamane Y, et al. Triggering the interferon response: the role of IRF-3 transcription factor. J Interferon Cytokine Res 1999;19:1–13.
19. Hinoshita E, Taguchi K, Inokuchi A, Uchiumi T, Kinukawa N, Shimada M, et al. Decreased expression of an ATP-binding cassette transporter, MRP2, in human livers with hepatitis C virus infection. J Hepatol 2001; 35:765–773.
20. Tanaka T, Uchiumi T, Hinoshita E, Inokuchi A, Toh S, Wada M, et al. The human multidrug resistance protein 2 gene: functional characterization of the 5′-flanking region and expression in hepatic cells. HEPATOLOGY 1999;30:1507–1512.
21. Inokuchi A, Hinoshita E, Iwamoto Y, Kohno K, Kuwano M, Uchiumi T. Enhanced expression of the human multidrug resistance protein 3 by bile salt in human enterocytes. A transcriptional control of a plausible bile acid transporter. J Biol Chem 2001;276:46822–46829.
22. Saklatvala J, Dean J, Finch A. Protein kinase cascades in intracellular signalling by interleukin-I and tumour necrosis factor. Biochem Soc Sympos 1999;64:63–77.
23. Moshage H. Cytokines and the hepatic acute phase response. J Pathol 1997;181:257–266.
24. Darnell JE Jr, Kerr IM, Stark GR. Jak-STAT pathways and transcriptional activation in response to IFNs and other extracellular signaling proteins. Science 1994;264:1415–1421.
25. Ihle JN, Kerr IM. Jaks and Stats in signaling by the cytokine receptor superfamily. Trends Genet 1995;11:69–74.
26. Servant MJ, Grandvaux N, Hiscott J. Multiple signaling pathways leading to the activation of interferon regulatory factor 3. Biochem Pharmacol 2002;64:985–992.
27. Trauner M, Fickert P, Stauber RE. Inflammation-induced cholestasis. J Gastroenterol Hepatol 1999;14:946–959.
28. Jansen PL, Roskams T. Why are patients with liver disease jaundiced? ATP-binding cassette transporter expression in human liver disease. J Hepatol 2001;35:811–813.
29. Trauner M, Arrese M, Lee H, Boyer JL, Karpen SJ. Endotoxin downregulates rat hepatic ntcp gene expression via decreased activity of critical transcription factors. J Clin Invest 1998;101:2092–2100.
30. Crawford JM, Boyer JL. Clinicopathology conferences: inflammation-induced cholestasis. HEPATOLOGY 1998;28:253–260.
31. Bolder U, Ton-Nu HT, Schteingart CD, Frick E, Hofmann AF. Hepatocyte transport of bile acids and organic anions in endotoxemic rats: impaired uptake and secretion. Gastroenterology 1997;112:214–225.
32. Denson LA, Auld KL, Schiek DS, McClure MH, Mangelsdorf DJ, Karpen SJ. Interleukin-1beta suppresses retinoid transactivation of two hepatic transporter genes involved in bile formation. J Biol Chem 2000;275:8835–8843.
33. Li D, Zimmerman TL, Thevananther S, Lee HY, Kurie JM, Karpen SJ. Interleukin-1 beta-mediated suppression of RXR:RAR transactivation of the Ntcp promoter is JNK-dependent. J Biol Chem 2002;277: 31416–31422.
34. Kast HR, Goodwin B, Tarr PT, Jones SA, Anisfeld AM, Stoltz CM, et al. Regulation of multidrug resistance-associated protein 2 (ABCC2) by the nuclear receptors pregnane X receptor, farnesoid X-activated receptor, and constitutive androstane receptor. J Biol Chem 2002;277:2908–2915.
35. Navarro L, Mowen K, Rodems S, Weaver B, Reich N, Spector D, et al. Cytomegalovirus activates interferon immediate-early response gene expression and an interferon regulatory factor 3-containing interferon-stimulated response element-binding complex. Mol Cell Biol 1998;18:3796–3802.

Direct inhibition of EGF receptor activation in vascular endothelial cells by gefitinib ('Iressa', ZD1839)

Akira Hirata,[1,2] Hisanori Uehara,[3] Keisuke Izumi,[3] Seiji Naito,[2] Michihiko Kuwano[4] and Mayumi Ono[1,5]

Departments of [1]Medical Biochemistry and [2]Urology, Graduate School of Medical Science, Kyushu University, 3-1-1 Maidashi, Higashi-ku, Fukuoka 812-8582; [3]Second Department of Pathology, The University of Tokushima School of Medicine, 2-50-1 Kuramotocho, Tokushima 770-0042; and [4]Research Center for Innovative Cancer Therapy of the 21st Century COE Program for Medical Science, Kurume University School of Medicine, 67 Asahimachi, Kurume 830-0011

(Received March 1, 2004/Revised May 8, 2004/Accepted May 24, 2004)

The development of gefitinib ('Iressa', ZD1839) by targeting the EGFR tyrosine kinase is a recent therapeutic highlight. We have reported that gefitinib is antiangiogenic *in vitro*, as well as *in vivo*. In this study, we asked if the anti-angiogenic action of gefitinib is due to a direct effect on activation of vascular endothelial cells by EGF. EGF, as well as VEGF, caused pronounced angiogenesis in an avascular area of the mouse cornea, and i.p. administration of gefitinib almost completely blocked the response to EGF, but not to VEGF. Immunohistochemical analysis demonstrated phosphorylation of EGFR by EGF in the neovasculature, and gefitinib markedly reduced this effect. Gefitinib also inhibited downstream activation of ERK 1/2 via EGFR in cultured microvascular endothelial (HMVE) cells. These findings suggest that the anti-angiogenic effect of gefitinib in the vascular endothelial cells of neo-vasculature is partly attributable to direct inhibition of EGFR activation, and that endothelial cells in malignant tumors play a critical role in the cancer therapeutic efficacy of gefitinib. (Cancer Sci 2004; 95: 614–618)

Protein tyrosine kinases play key roles in cell proliferation, cell death, development, differentiation, cell motility, morphogenesis, and angiogenesis.[1,2] The ErbB-family protein kinases are important representatives of this type of protein kinase, and their signaling network in development and differentiation has been well studied.[3,4] In particular, expression of the EGFR and other ErbB-family proteins is often associated with stimulation of cell growth and apoptosis in cancer. A recent therapeutic highlight is the development of targeted anticancer drugs, such as gefitinib ('Iressa', ZD1839) and herceptin, that inhibit ErbB-family tyrosine kinases.[5,6] Gefitinib is an orally active EGFR tyrosine kinase inhibitor that blocks signal transduction pathways implicated in cancer growth, and decreases cellular proliferation, angiogenesis, tumor invasion and metastasis while increasing apoptosis.[7–10] Gefitinib has anti-proliferation activity in various human cancer cell types *in vivo* as well as *in vitro*,[11,12] and is also effective in cancer patients.[7] Our recent study has demonstrated that sensitivity to gefitinib in non-small cell lung cancer cell lines is associated with dependence on Akt and ERK 1/2 activation in response to EGFR signaling.[13]

We have previously reported that gefitinib can inhibit angiogenesis *in vivo* as well as *in vitro*: it inhibited both EGF-induced migration of HMVE cells and EGF-induced neovascularization in the mouse cornea.[14] Angiogenesis is often provoked by the major pro-angiogenic factors, bFGF, VEGF, IL-8, PDGF, and EGF/TGFα.[15–17] The stimulatory effect of EGF/TGFα in angiogenesis is, however, not yet well understood. We have reported that EGF/TGFα-induced angiogenesis might be attributable to its signaling through direct interaction with vascular endothelial cells,[14,18] and also to angiogenesis-related factors that are produced from cancer cells and vascular endothelial cells, based on studies using various angiogenesis models.[14,19,20] However, it remains unclear whether EGF-induced angiogenesis *in vivo* is mediated by direct interaction with endothelial cells. The vascular endothelial cells in a number of tumor types are known to express EGFR,[21–23] and suppression of VEGF or EGF expression inhibited the growth of a wide variety of tumor types in a murine tumor model, while angiogenesis inhibitors that target VEGF receptor or EGFR reduced tumor growth, metastasis, and the microvessel density of human pancreatic cancer in nude mice.[24] In addition, blockade of EGFR by a tyrosine kinase inhibitor can suppress both EGFR-induced proliferation in cancer, and EGFR-induced survival of tumor-associated endothelial cells in an animal model.[25,26] The tyrosine kinase inhibitor also blocked activation of EGFR in tumor-associated endothelial cells. Taken together, these results indicate that EGFR is activated in response to EGF, TGFα, and other ligands that are secreted into the tumor microenvironment.

In the present study, we asked if gefitinib inhibits angiogenesis in vascular endothelial cells by interfering with EGFR activation, or by inhibiting the EGF/TGFα-induced expression of other potent angiogenic factors, such as VEGF and IL-8, as suggested by others.[27,28] We first present findings in the mouse cornea that point to direct involvement of EGF/EGFR signaling in angiogenesis by the vascular endothelial cells in EGF-induced neo-vasculature, and then present evidence that the anti-angiogenic effect of gefitinib is partly attributable to direct inhibition of EGFR activation in neo-vasculature by EGF.

Materials and Methods

Materials. Gefitinib was kindly provided by AstraZeneca (Macclesfield, UK). Murine EGF was purchased from Toyobo (Osaka, Japan) and recombinant mouse VEGF from R&D Systems, Inc. (Minneapolis, MN). Anti-EGFR antibody and anti-phospho-EGFR antibody were purchased from Upstate Biotechnology (Lake Placid, NY). Antibodies to ERK 1/2, phospho-ERK 1/2, Akt, and phospho-Akt were from Cell Signaling Technology (Beverly, MA).

Cell culture. HMVE cells derived from neonatal dermis (Cascade Biologics, Portland, OR) were cultured in medium 131 containing microvascular growth supplement (Cascade Biologics). We used cells at passage 3–4 after recovery from frozen stocks. The cells were maintained under standard cell culture conditions at 37°C and 5% CO_2 in a humid environment.

[5]To whom correspondence should be addressed.
E-mail: mayumi@biochem1.med.kyushu-u.ac.jp

Abbreviations: Akt, protein kinase B/Akt; bFGF, basic fibroblast growth factor; EGF, epidermal growth factor; EGFR, epidermal growth factor receptor; ERK, extracellular signal-regulated kinase; HMVE cells, human microvascular endothelial cells; IL-8, interleukin-8; TGFα, transforming growth factor α; VEGF, vascular endothelial growth factor.

'Iressa' is a trademark of the AstraZeneca group of companies.

Western blot analysis. HMVE cells were cultured in medium containing 1% FBS for 12 h, then incubated with 0 to 5 μ*M* gefitinib for 3 h before stimulation with 20 ng/ml EGF or 20 ng/ml VEGF for 10 min at 37°C. They were rinsed with ice-cold PBS then lysed in Triton X-100 buffer (50 μ*M* HEPES, 150 μ*M* NaCl, 1% Triton X-100 and 10% glycerol containing 1 m*M* PMSF, 10 μg/ml aprotinin, 10 μg/ml leupeptin and 1 m*M* sodium vanadate). Lysates were subjected to SDS polyacrylamide gel electrophoresis and transferred to Immobilon membranes (Millipore, Bedford, MA). Blots were incubated with blocking solution and probed with anti-EGFR antibody, anti-phospho-EGFR antibody, anti-ERK 1/2 antibody, anti-phospho-ERK 1/2 antibody, anti-Akt antibody and anti-phospho-Akt antibody, followed by washing. Antigen-antibody complexes were then visualized with horseradish peroxidase-conjugated secondary antibodies following by enhanced chemiluminescence (ECL; Amersham, Piscataway, NJ), as described previously.[14, 29]

Corneal micropocket assay in mice and quantification of corneal neo-vascularization. The corneal micropocket assay was performed essentially as previously described.[14, 30] Briefly, 0.3 μl of Hydron pellets (IFN Sciences, New Brunswick, NI) containing murine EGF (200 ng) or murine VEGF (200 ng) were implanted into the corneas of male BALB/c mice, and gefitinib was administered by i.p. injection (100 mg/kg/day) on days 1–5. On day 6, mice were sacrificed and their corneal vessels were photographed. Images of the corneas were recorded using Nikon Coolscan software with standardized illumination, contrast, and threshold settings, and were saved on disk. Areas of corneal neo-vascularization were analyzed using the software package NIH Image 1.61, and expressed in mm^2.

Immunofluorescence double staining for CD31/PECAM-1 and EGFR or phospho-EGFR (Tyr845). Frozen sections were fixed in cold acetone for 10 min. After having been rinsed three times for 3 min each with PBS, sections that had been immunostained for CD31/EGF-R and CD31/phospho-EGFR were incubated with a 1:100 dilution of monoclonal rat anti-mouse CD31/PECAM-1 antibody (PharMingen, San Diego, CA) containing 5% normal goat serum for 1 h at room temperature. The sections were rinsed again three times for 3 min each with PBS, then incubated with a 1:400 dilution of secondary Alexa 594-conjugated goat anti-rat IgG antibody (Molecular Probes, Eugene, OR) for 1 h at room temperature in the dark. Samples were then rinsed three times with PBS, and incubated at 4°C for 18 h with a 1:50 dilution of polyclonal rabbit anti-human EGFR antibody (Santa Cruz Biotechnology, Santa Cruz, CA) and a 1:50 dilution of polyclonal rabbit anti-phospho-EGFR (Tyr845) antibody (Cell Signaling Technology), both of which are mouse cross-reactive. The samples were further rinsed three times for 3 min each with PBS, then incubated with a 1:400 dilution of secondary Alexa 488-conjugated goat anti-rabbit IgG (Molecular Probes) for 1 h at room temperature in the dark. The samples were then rinsed three times for 5 min each with PBS and mounted with Vectashield (Vector Laboratories, Inc., Burlingame, CA). Immunofluorescence microscopy was performed using a ×20 objective. The images were captured using a CoolSNAP camera, Epifluorescence upright microscopy system (Olympus Optical Co., Ltd., Tokyo), and MetaCam software (Universal Imaging Corporation, Downingtown, PA).

Statistical analysis. Statistical comparisons were performed using the Mann-Whitney test; $P<0.05$ was considered significant.

Results

Gefitinib inhibits EGF-induced angiogenesis but not VEGF-induced angiogenesis. We first examined if EGF or VEGF could induce angiogenesis in the mouse cornea. Administration of EGF or VEGF in Hydron pellets induced marked angiogenesis in an avascular area of the cornea (Fig. 1, A and C), consistent with our previous study.[14] I.p. administration of gefitinib blocked EGF-induced neo-vascularization, but not VEGF-induced neovascularization. Quantitative analysis using four mice in each assay consistently showed more than 70% inhibition of EGF-induced neo-vascularization by gefitinib, and almost no inhibition of VEGF-induced neo-vascularization (Fig. 1B).

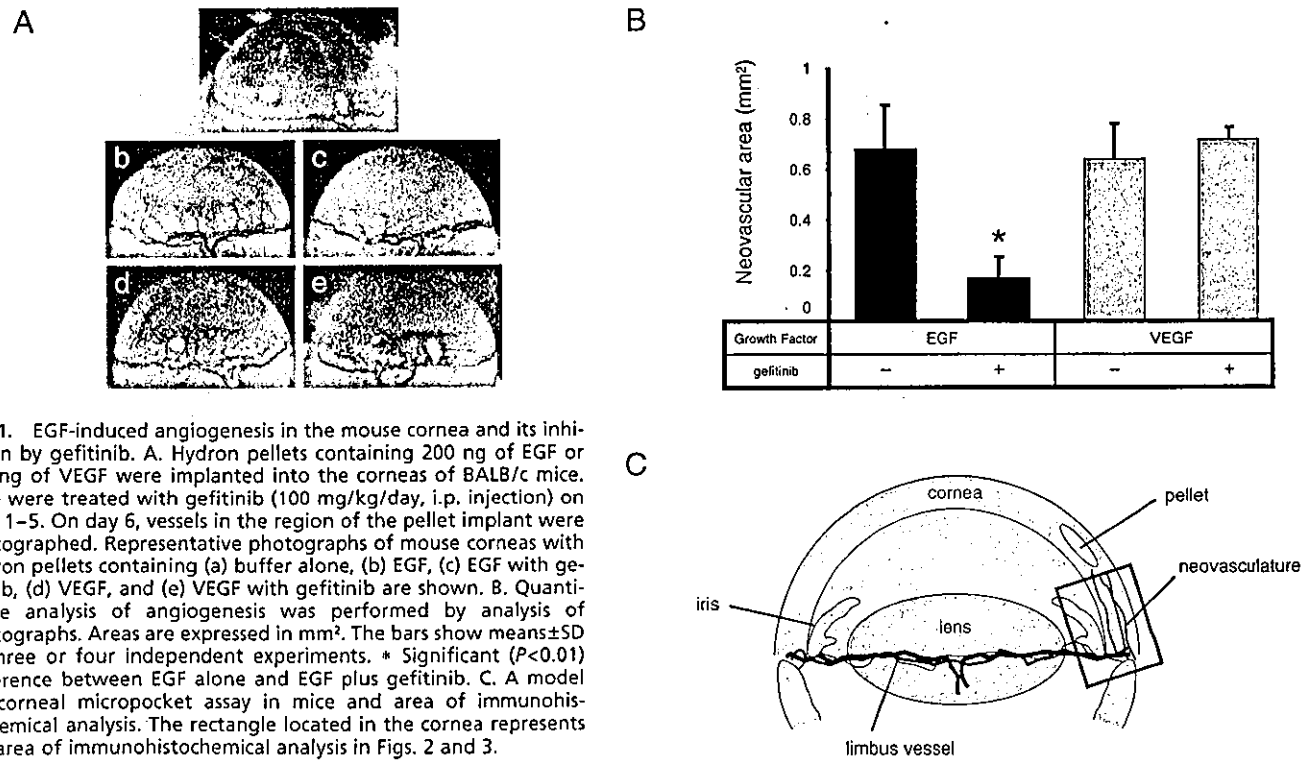

Fig. 1. EGF-induced angiogenesis in the mouse cornea and its inhibition by gefitinib. A. Hydron pellets containing 200 ng of EGF or 200 ng of VEGF were implanted into the corneas of BALB/c mice. Mice were treated with gefitinib (100 mg/kg/day, i.p. injection) on days 1–5. On day 6, vessels in the region of the pellet implant were photographed. Representative photographs of mouse corneas with Hydron pellets containing (a) buffer alone, (b) EGF, (c) EGF with gefitinib, (d) VEGF, and (e) VEGF with gefitinib are shown. B. Quantitative analysis of angiogenesis was performed by analysis of photographs. Areas are expressed in mm^2. The bars show means±SD of three or four independent experiments. * Significant ($P<0.01$) difference between EGF alone and EGF plus gefitinib. C. A model for corneal micropocket assay in mice and area of immunohistochemical analysis. The rectangle located in the cornea represents the area of immunohistochemical analysis in Figs. 2 and 3.

Gefitinib inhibits EGF-induced EGFR activation in EGF-induced neovasculature. To determine whether gefitinib inhibits EGFR phosphorylation in endothelial cells, we performed an immunohistochemical analysis of the corneal micropocket of mice. Cross sections of cornea exposed to EGF or VEGF in the area exhibited in Fig. 1C showed the development of extensive CD31-positive neo-vasculature (Fig. 2). Some EGFR-positive cells were observed in the CD31-positive vascular endothelial cells in corneas induced by EGF or VEGF whether or not gefitinib was present (Fig. 2). However, the number of EGFR-positive vascular endothelial cells in vasculature induced by VEGF was somewhat smaller than that in the case of EGF. By contrast, there were few, if any, EGFR-positive cells in the control untreated group.

We next examined whether the EGFR in the EGF-induced corneal neo-vasculatures was phosphorylated. To our surprise, we found many endothelial cells in neo-vasculature induced by EGF, but not that induced by VEGF, stained positively for phosphorylated EGFR (Fig. 3). More than 50% of endothelial cells were phospho-EGFR positive. Daily i.p. administration of gefitinib resulted in reduced numbers of phospho-EGFR-positive cells with a concomitant decrease in corneal angiogenesis (Fig. 3). Gefitinib however did not affect the development of neo-vasculature, or the phosphorylation state of EGFR, in response to VEGF.

Gefitinib inhibits EGF-induced, but not VEGF-induced activation of ERK 1/2 *in vitro*. We previously reported that EGFR phosphorylation and EGF-activated signaling were inhibited by gefitinib in EGFR-expressing HMVE cells derived from human omentum.[14] In our present study, we examined if EGF/EGFR signaling was activated in another type of HMVE cells derived from neonatal dermis with very low levels of EGFR. Both Akt and ERK 1/2 were phosphorylated by EGF in these HMVE cells (Fig. 4A). Moreover, gefitinib at 0.1 μM almost completely inhibited EGF-induced activation of ERK 1/2, while at 5 μM it reduced Akt phosphorylation to the untreated control level (Fig.

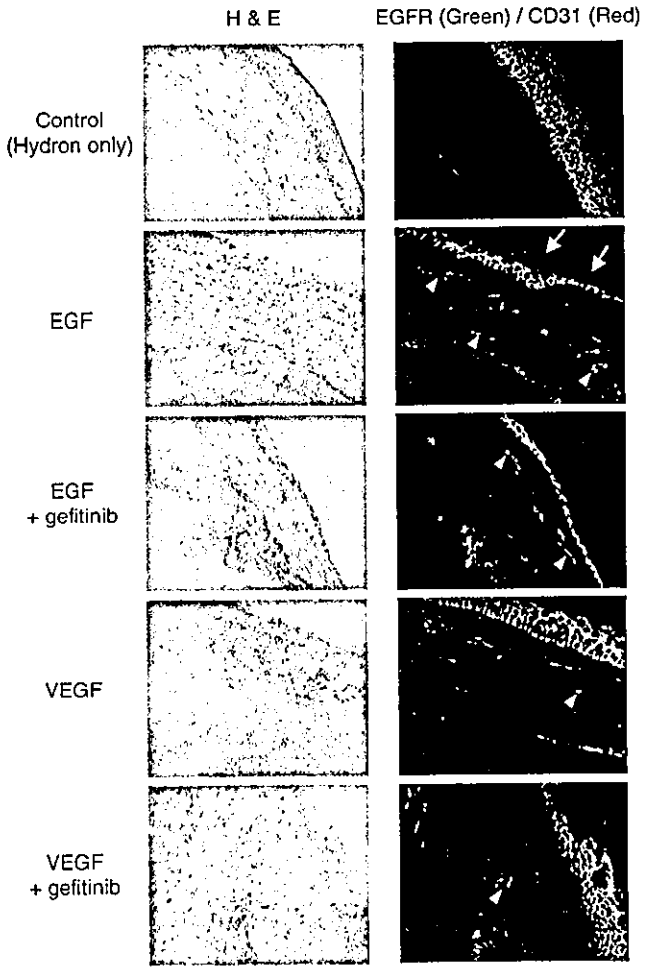

Fig. 2. Immunohistochemically stained mouse cornea sections and expression of EGFR and CD31 in the presence or absence of EGF or VEGF with or without gefitinib treatment. EGFR (green) and CD31 (red) were immunostained with specific antibodies in mouse cornea sections. CD31-positive cells are indicative of EGF or VEGF-induced neo-vasculature in the cornea. Hematoxylin-eosin (H&E) staining of counterparts of each stained sample is shown in the left panel. In the photograph of cornea exposed to EGF: white arrow, epithelial layer in cornea; white arrowhead, neo-vasculature in corneal stromal layer. ×400.

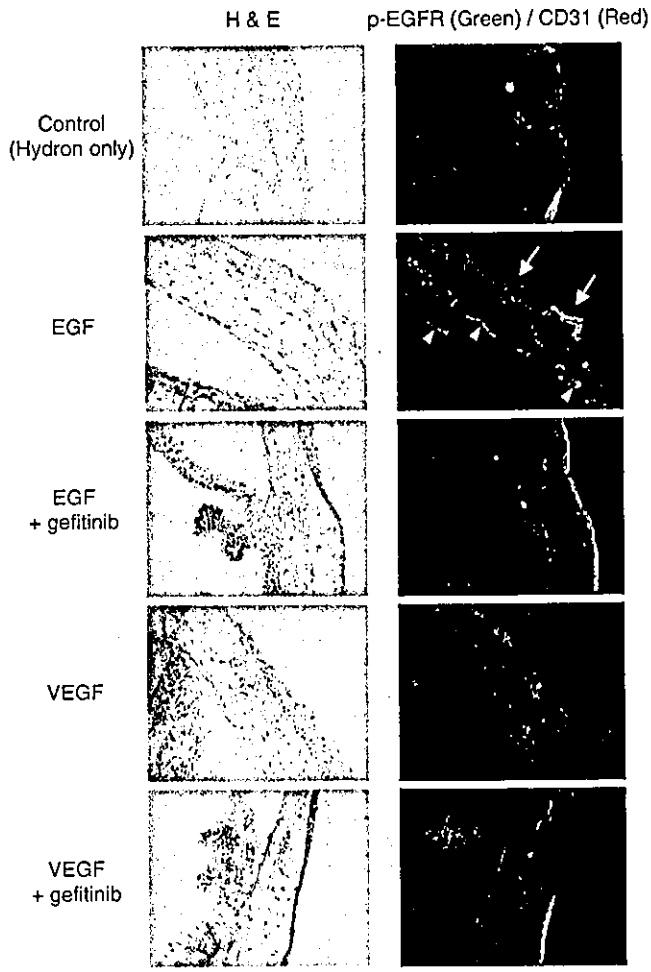

Fig. 3. EGF-induced EGFR phosphorylation of neo-vasculature in mouse corneas and inhibition by gefitinib. Immunohistochemical analysis was performed on mouse cornea sections with specific antibodies against CD31 (red) and phosphorylated EGFR (green). Many endothelial cells in the neo-vasculature are positive for phosphorylated EGFR (merged, yellow) after stimulation with EGF, and i.p. administration of gefitinib diminishes the appearance of such phosphorylated EGFR-positive cells. In contrast, almost no cells positive for phosphorylated EGFR were observed in neo-vasculature formed in response to VEGF with or without administration of gefitinib. Hematoxylin-eosin (H&E) staining of counterparts of each stained sample is shown in the left panel. In the photograph of cornea exposed to EGF: white arrow, epithelial layer in cornea; white arrowhead, neovasculature in corneal stromal layer. ×400.

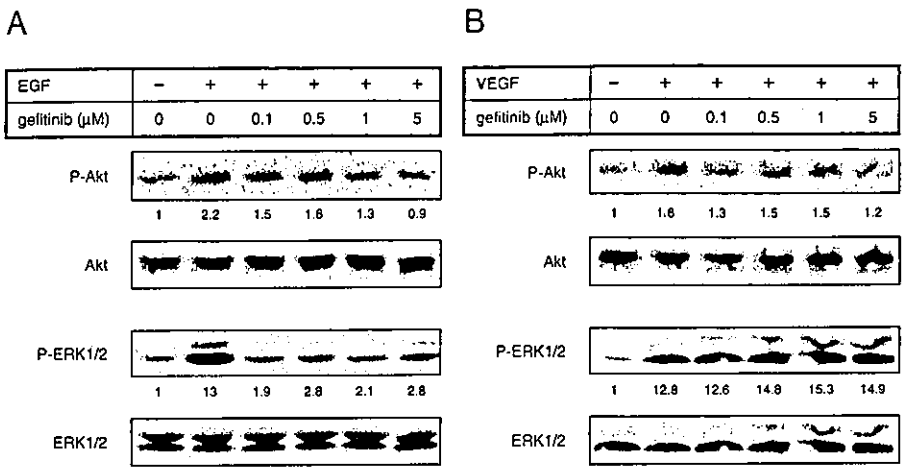

Fig. 4. Inhibition of EGF-induced but not VEGF-induced activation of Akt and ERK 1/2 by gefitinib in HMVE cells. Serum-starved HMVE cells were treated for 3 h with gefitinib, followed by (A) EGF (20 ng/ml) or (B) VEGF (20 ng/ml) for 10 min. Protein extracts were resolved by SDS-PAGE and probed with specific antibodies. Akt and ERK 1/2 activities were determined with anti-phospho-Akt and anti-phospho-ERK 1/2 antibodies, and the immunoreactive proteins were visualized by means of enhanced chemiluminescence. Activities of phosphorylated Akt and ERK 1/2 are normalized to their activities in the absence of EGF or VEGF.

4A). We could detect a small amount of EGFR in these cells by western blot analysis, but failed to detect any phosphorylation of EGFR with antibody against phosphorylated EGFR (data not shown). As shown in Fig. 4B, both Akt and ERK 1/2 were also activated by VEGF in HMVE cells. However, gefitinib could not inhibit this activation by VEGF.

Discussion

We have shown that EGF is as potent as VEGF in inducing angiogenesis in a mouse cornea assay, in agreement with our previous study.[14] Both indirect and direct mechanisms have been considered to underlie EGF/TGFα-induced angiogenesis: on the one hand, EGF/TGFα secreted by tumor cells and/or tumor stoma cells enhanced the production of potent angiogenic factors, such as VEGF, IL-8, and metalloproteinases, resulting in angiogenesis via the paracrine and/or autocrine route[31-33]; on the other hand, activation of EGFR expressed in neo-vasculature in response to EGF/TGFα induced an angiogenic switch of the endothelial cells.[18,20,22] Concerning the latter direct mechanism, some dividing endothelial cells have been shown to express EGFR.[21,23,34] In addition, Fidler and colleagues have recently reported that tumor-associated endothelial cells express activated EGFR, and also that administration of EGFR tyrosine kinase inhibitors decreases this EGFR activation, with concomitant inhibition of tumor growth and/or metastasis and induction of apoptosis of the endothelial cells.[25,26,35] We also demonstrated above a marked decrease in the number of vascular endothelial cells with phosphorylated EGFR in response to gefitinib. In contrast, gefitinib had almost no effect on VEGF-induced neo-vascularization. We may therefore conclude that, in the present *in vivo* model, activated EGFR is directly involved in angiogenesis in response to EGF. In agreement with this notion, we also observed that gefitinib inhibits downstream activation of ERK 1/2 by EGF/EGFR *in vitro* (see Fig. 4A).

Activation of MAPK and Akt in vascular endothelial cells appears to be essential for angiogenesis. Kim *et al.*[36] have reported that betacellulin, a member of the EGF family, has an angiogenic effect in the Matrigel plug assay, and that it activates ERK 1/2 and Akt in human umbilical vascular endothelial cells. We have also shown that EGF activates MAPK and Akt in HMVE cells derived from neonatal dermis *in vitro* (this study) as well as in HMVE cells derived from the omentum.[14] Gefitinib caused rather more inhibition of the activation of ERK 1/2 than of Akt, and it is possible that activation of ERK 1/2 in vascular endothelial cells is more closely associated with the EGF-induced angiogenesis switch than is activation of Akt. However, this matter needs further clarification.

Both EGF and EGFR are expressed in the corneal epithelium,[37] and systemic administration of gefitinib not only delayed the healing of a corneal epithelial wound, but also reduced the thickness of unwounded corneal epithelium.[38] This suggests that EGFR plays a key role in corneal wound healing and homeostasis of the corneal epithelium. We also observed expression of EGFR, and its activation, in the corneal epithelium (Figs. 2 and 3). Whereas activation of EGFR in the neovasculature of the corneal stroma was highly susceptible to inhibition of gefitinib, activation of EGFR in the corneal epithelium appeared to be resistant. It may be that EGF/EGFR levels and activation of EGFR are not responsive to environmental stimuli and poisons in the corneal epithelium. Alternatively, the corneal epithelium may possess homeostatic mechanisms of the kind demonstrated by Wilson *et al.*,[39] or be protected by the corneal blood-epithelium barrier.

In conclusion, EGF/TGFα and related ligands are produced by many types of tumors. The antitumor effect of gefitinib and other EGFR tyrosine kinase inhibitors appears to be partly attributable to their anti-angiogenic activities via direct inhibition of EGFR activation in neo-vasculature in response to these ligands.

This study was supported by a grant-in-aid for cancer research from the Ministry of Education, Culture, Sports, Science and Technology, Japan, and also by a cancer research grant from the Ministry of Health, Labour and Welfare, Japan.

1. Ullrich A, Schlessinger J. Signal transduction by receptors with tyrosine kinase activity. *Cell* 1990; 61: 203–12.
2. Yarden Y, Ullrich A. Growth factor receptor tyrosine kinases. *Annu Rev Biochem* 1988; 57: 443–78.
3. Olayioye MA, Neve RM, Lane HA, Hynes NE. The ErbB signaling network: receptor heterodimerization in development and cancer. *EMBO J* 2000; 19: 3159–67.
4. Prenzel N, Fischer OM, Streit S, Hart S, Ullrich A. The epidermal growth factor receptor family as a central element for cellular signal transduction and diversification. *Endocr Relat Cancer* 2001; 8: 11–31.

5. Baselga J. Why the epidermal growth factor receptor? The rationale for cancer therapy. *Oncologist* 2002; 7 Suppl 4: 2–8.
6. Mendelsohn J, Baselga J. The EGF receptor family as targets for cancer therapy. *Oncogene* 2000; **19**: 6550–65.
7. Baselga J, Averbuch SD. ZD1839 ('Iressa') as an anticancer agent. *Drugs* 2000; **60** Suppl 1: 33–40; discussion 41-32.
8. Barker AJ, Gibson KH, Grundy W, Godfrey AA, Barlow JJ, Healy MP, Woodburn JR, Ashton SE, Curry BJ, Scarlett L, Henthorn L, Richards L. Studies leading to the identification of ZD1839 (IRESSA): an orally active, selective epidermal growth factor receptor tyrosine kinase inhibitor targeted to the treatment of cancer. *Bioorg Med Chem Lett* 2001; **11**: 1911–4.
9. Arteaga CL, Johnson DH. Tyrosine kinase inhibitors—ZD1839 (Iressa). *Curr Opin Oncol* 2001; **13**: 491–8.
10. Woodburn JR. The epidermal growth factor receptor and its inhibition in cancer therapy. *Pharmacol Ther* 1999; **82**: 241–50.
11. Ciardiello F, Caputo R, Bianco R, Damiano V, Pomatico G, De Placido S, Bianco AR, Tortora G. Antitumor effect and potentiation of cytotoxic drugs activity in human cancer cells by ZD-1839 (Iressa), an epidermal growth factor receptor-selective tyrosine kinase inhibitor. *Clin Cancer Res* 2000; **6**: 2053–63.
12. Sirotnak FM, Zakowski MF, Miller VA, Scher HI, Kris MG. Efficacy of cytotoxic agents against human tumor xenografts is markedly enhanced by coadministration of ZD1839 (Iressa), an inhibitor of EGFR tyrosine kinase. *Clin Cancer Res* 2000; **6**: 4885–92.
13. Ono M, Hirata A, Kometani T, Miyagawa M, Ueda S, Kinoshita H, Fujii T, Kuwano M. Sensitivity to gefitinib (Iressa, ZD1839) in non-small cell lung cancer cell lines correlates with dependence on the EGF receptor/ERK1/2 and EGF receptor/Akt pathway for proliferation. *Mol Cancer Ther* 2004; **3**: 465–72.
14. Hirata A, Ogawa S, Kometani T, Kuwano T, Naito S, Kuwano M, Ono M. ZD1839 (Iressa) induces antiangiogenic effects through inhibition of epidermal growth factor receptor tyrosine kinase. *Cancer Res* 2002; **62**: 2554–60.
15. Klagsbrun M, D'Amore PA. Regulators of angiogenesis. *Annu Rev Physiol* 1991; **53**: 217–39.
16. Hanahan D, Folkman J. Patterns and emerging mechanisms of the angiogenic switch during tumorigenesis. *Cell* 1996; **86**: 353–64.
17. Kuwano M, Fukushi J, Okamoto M, Nishie A, Goto H, Ishibashi T, Ono M. Angiogenesis factors. *Intern Med* 2001; **40**: 565–72.
18. Ono M, Okamura K, Nakayama Y, Tomita M, Sato Y, Komatsu Y, Kuwano M. Induction of human microvascular endothelial tubular morphogenesis by human keratinocytes: involvement of transforming growth factor-alpha. *Biochem Biophys Res Commun* 1992; **189**: 601–9.
19. Sato Y, Okamura K, Morimoto A, Hamanaka R, Hamaguchi K, Shimada T, Ono M, Kohno K, Sakata T, Kuwano M. Indispensable role of tissue-type plasminogen activator in growth factor-dependent tube formation of human microvascular endothelial cells *in vitro*. *Exp Cell Res* 1993; **204**: 223–9.
20. Mawatari M, Okamura K, Matsuda T, Hamanaka R, Mizoguchi H, Higashio K, Kohno K, Kuwano M. Tumor necrosis factor and epidermal growth factor modulate migration of human microvascular endothelial cells and production of tissue-type plasminogen activator and its inhibitor. *Exp Cell Res* 1991; **192**: 574–80.
21. Schreiber AB, Winkler ME, Derynck R. Transforming growth factor-alpha: a more potent angiogenic mediator than epidermal growth factor. *Science* 1986; **232**: 1250–3.
22. Goldman CK, Kim J, Wong WL, King V, Brock T, Gillespie GY. Epidermal growth factor stimulates vascular endothelial growth factor production by human malignant glioma cells: a model of glioblastoma multiforme pathophysiology. *Mol Biol Cell* 1993; **4**: 121–33.
23. Rockwell P, O'Connor WJ, King K, Goldstein NI, Zhang LM, Stein CA. Cell-surface perturbations of the epidermal growth factor and vascular endothelial growth factor receptors by phosphorothioate oligodeoxynucleotides. *Proc Natl Acad Sci USA* 1997; **94**: 6523–8.
24. Baker CH, Solorzano CC, Fidler IJ. Blockade of vascular endothelial growth factor receptor and epidermal growth factor receptor signaling for therapy of metastatic human pancreatic cancer. *Cancer Res* 2002; **62**: 1996–2003.
25. Baker CH, Kedar D, McCarty MF, Tsan R, Weber KL, Bucana CD, Fidler IJ. Blockade of epidermal growth factor receptor signaling on tumor cells and tumor-associated endothelial cells for therapy of human carcinomas. *Am J Pathol* 2002; **161**: 929–38.
26. Kim SJ, Uehara H, Karashima T, Shepherd DL, Killion JJ, Fidler IJ. Blockade of epidermal growth factor receptor signaling in tumor cells and tumor-associated endothelial cells for therapy of androgen-independent human prostate cancer growing in the bone of nude mice. *Clin Cancer Res* 2003; **9**: 1200–10.
27. Kerbel RS, Viloria-Petit A, Okada F, Rak J. Establishing a link between oncogenes and tumor angiogenesis. *Mol Med* 1998; **4**: 286–95.
28. de Jong JS, van Diest PJ, van der Valk P, Baak JP. Expression of growth factors, growth-inhibiting factors, and their receptors in invasive breast cancer. II: Correlations with proliferation and angiogenesis. *J Pathol* 1998; **184**: 53–7.
29. Nakao S, Kuwano T, Ishibashi T, Kuwano M, Ono M. Synergistic effect of TNF-alpha in soluble VCAM-1-induced angiogenesis through alpha(4) integrins. *J Immunol* 2003; **170**: 5704–11.
30. Gimbrone MA Jr, Gullino PM. Neovascularization induced by intraocular xenografts of normal, preneoplastic, and neoplastic mouse mammary tissues. *J Natl Cancer Inst* 1976; **56**: 305–18.
31. Benjamin LE, Keshet E. Conditional switching of vascular endothelial growth factor (VEGF) expression in tumors: induction of endothelial cell shedding and regression of hemangioblastoma-like vessels by VEGF withdrawal. *Proc Natl Acad Sci USA* 1997; **94**: 8761–6.
32. Kitadai Y, Haruma K, Sumii K, Yamamoto S, Ue T, Yokozaki H, Yasui W, Ohmoto Y, Kajiyama G, Fidler IJ, Tahara E. Expression of interleukin-8 correlates with vascularity in human gastric carcinomas. *Am J Pathol* 1998; **152**: 93–100.
33. Bancroft CC, Chen Z, Yeh J, Sunwoo JB, Yeh NT, Jackson S, Jackson C, Van Waes C. Effects of pharmacologic antagonists of epidermal growth factor receptor, PI3K and MEK signal kinases on NF-kappaB and AP-1 activation and IL-8 and VEGF expression in human head and neck squamous cell carcinoma lines. *Int J Cancer* 2002; **99**: 538–48.
34. Bohling T, Hatva E, Kujala M, Claesson-Welsh L, Alitalo K, Haltia M. Expression of growth factors and growth factor receptors in capillary hemangioblastoma. *J Neuropathol Exp Neurol* 1996; **55**: 522–7.
35. Bruns CJ, Solorzano CC, Harbison MT, Ozawa S, Tsan R, Fan D, Abbruzzese J, Traxler P, Buchdunger E, Radinsky R, Fidler IJ. Blockade of the epidermal growth factor receptor signaling by a novel tyrosine kinase inhibitor leads to apoptosis of endothelial cells and therapy of human pancreatic carcinoma. *Cancer Res* 2000; **60**: 2926–35.
36. Kim HS, Shin HS, Kwak HJ, Cho CH, Lee CO, Koh GY. Betacellulin induces angiogenesis through activation of mitogen-activated protein kinase and phosphatidylinositol 3'-kinase in endothelial cell. *FASEB J* 2003; **17**: 318–20.
37. Wilson SE, Schultz GS, Chegini N, Weng J, He YG. Epidermal growth factor, transforming growth factor alpha, transforming growth factor beta, acidic fibroblast growth factor, basic fibroblast growth factor, and interleukin-1 proteins in the cornea. *Exp Eye Res* 1994; **59**: 63–71.
38. Nakamura Y, Sotozono C, Kinoshita S. The epidermal growth factor receptor (EGFR): role in corneal wound healing and homeostasis. *Exp Eye Res* 2001; **72**: 511–7.
39. Wilson SE, Chen L, Mohan RR, Liang Q, Liu J. Expression of HGF, KGF, EGF and receptor messenger RNAs following corneal epithelial wounding. *Exp Eye Res* 1999; **68**: 377–97.

GLIA 47:325–334 (2004)

N-myc Downstream-Regulated Gene 1 Expression in Injured Sciatic Nerves

KAZUHO HIRATA,[1]* KATSUAKI MASUDA,[2] WATARU MORIKAWA,[2] JIAN-WEN HE,[1] AKIO KURAOKA,[1] MICHIHIKO KUWANO,[2] AND MASARU KAWABUCHI[1]
[1]*Department of Anatomy and Cell Biology, Graduate School of Medical Sciences, Kyushu University, Fukuoka, Japan*
[2]*Department of Medical Biochemistry, Graduate School of Medical Sciences, Kyushu University, Fukuoka, Japan*

KEY WORDS NDRG1; nerve regeneration; Schwann cells; immunohistochemistry

ABSTRACT N-myc downstream-regulated gene 1 (NDRG1)/RTP/Drg1/Cap43/rit42/TDD5/Ndr1 is expressed ubiquitously and has been proposed to play a role in growth arrest and cell differentiation. A recent study showed that mutation of this gene is responsible for hereditary motor and sensory neuropathy-Lom. However, the role of this gene in the peripheral nervous system is not fully understood. In our study, rabbit polyclonal antibodies were raised against this gene product and were used to examine changes in its expression over the time course of Wallerian degeneration and ensuing regeneration after crush injury of mouse sciatic nerves. Fluorescent immunohistochemistry showed that NDRG1 was expressed over the intact nerve fibers. Double labeling with a Schwann cell (SC) marker, S-100 protein (S-100), revealed that NDRG1 was localized in the cytoplasm of S-100-positive Schwann cells (SCs). NDRG1 expression was maintained in the early stage of myelin degradation but was then markedly depleted at the end stage of myelin degradation when frequent occurrence of BrdU-labeled SCs was observed (at 7–9 days). The depletion of NDRG1 at this time point was also confirmed by Western blotting analysis. NDRG1 expression finally recovered at the stage of remyelination, with immunoreactivity stronger than that in intact nerves. These findings suggest that NDRG1 may play an important role in the terminal differentiation of SCs during nerve regeneration.

INTRODUCTION

N-myc downstream-regulated gene 1 was originally designated reducing agent and tunicamycin-responsive protein (RTP) (Kokame et al., 1996), homologues of which were then isolated repeatedly: human differentiation-related gene 1 (Drg1) (van Belzen et al., 1997), human protein induced by free intracellular Ca^{2+} (Cap43) (Zhou et al., 1998), the mouse homologue designated TDD5 (Lin and Chang, 1997), reduced in tumor, p43 (rit42) (Kurdistani et al., 1998), and N-myc-downstream, repressed gene 1 (Ndr1) (Shimono et al., 1999). Currently the official name of this gene is NDRG1, determined by the HUGO Gene Nomenclature Committee (Qu et al., 2002). We have adopted the nomenclature NDRG1 in this report. A recent study showed that NDRG1 is a member of the NDRG gene family that contains an α/-β-hydrolase fold (Qu et al., 2002) without the residues required for catalysis (Shaw et al., 2002). It encodes a highly conserved protein with a high degree of homology to the proteins in other species, such as zebrafish (Gen Bank Accession Nos. AW281236 and AI657643), fruit flies (AF145604 and AE003454), nematodes (Z68135 and AL132847), sunflowers (Y09057 and AF189147) (Krauter-Canham et al., 1997), and *Arabidopsis* (AC005917 and AL163814). The evolutional conservation of this gene implies that it plays an important biological role. This gene has been reported to be involved in cell growth and differ-

*Correspondence to: Kazuho Hirata, Department of Anatomy and Cell Biology, Graduate School of Medical Sciences, Kyushu University, Higashi-ku, Maidashi 3-1-1, Fukuoka, 812-8582 Japan. E-mail: hirata@anat1.med.kyushu-u.ac.jp

Received 20 September 2003; Accepted 29 January 2004
DOI 10.1002/glia.20037
Published online 30 April 2004 in Wiley InterScience (www.interscience.wiley.com).

entiation (van Belzen et al., 1997; Piquemal et al., 1999; Shimono et al., 1999; Gomez-Casero et al., 2001), stress responses (Kokame et al., 1996; Xu et al., 1999; Agarwala et al., 2000; Salnikow et al., 2000; Segawa et al., 2002), and hormone responses (Lin and Chang, 1997; Ulrix et al., 1999; Segawa et al., 2002). Of particular interest is the observation that NDRG1 may have a complex but important function in carcinogenesis (Guan et al., 2000; Salnikow et al., 2000; Gomez-Casero et al., 2001; Nishie et al., 2001; Segawa et al., 2002; Bandyopadhyay et al., 2003) and atherogenesis (Kokame et al., 1996; Sato et al., 1998). Furthermore, attention has been drawn to the fact that this gene was identified as a gene responsible for hereditary motor and sensory neuropathy-Lom (HMSNL) (Kalaydjieva et al., 2000), which is an autosomal recessive form of Charcot-Marie-Tooth disease (CMT) and an early-onset peripheral neuropathy that progresses to severe disability in adulthood. However, the precise role of NDRG1 in the peripheral nervous system (PNS) remains to be elucidated.

It is well known that after axotomy the PNS has the capacity to be repaired by the established sequential process of Wallerian degeneration and ensuing regeneration (for review, see Hirata and Kawabuchi, 2002). Our previous studies (Hirata et al., 1999; Hirata et al., 2000, 2003) obtained stable and consistent results for the time course of the cellular and molecular events seen in the distal stump of the sciatic nerves following crush injury. It is expected that this crush injury model will provide useful clues for exploring the role of NDRG1 in the PNS. In the present study, polyclonal antibody (pAb) was raised against NDRG1 and was used for immunofluorescent labeling of mouse sciatic nerves after crush injury. The results showed that the expression of NDRG1, which was localized in the cytoplasm of Schwann cells (SCs) in intact nerves, dramatically changed during the process of regeneration. The role of the NDRG1 in the PNS is discussed.

MATERIALS AND METHODS

Production of Polyclonal Anti-NDRG1 Antisera

Synthetic peptides corresponding to internal sequences of human NDRG1 were prepared and used as immunogens. These included the TSEGTRSRSC sequence that corresponds to the tandem repetitive region unique to NDRG1 (Kokame et al., 1996; Okuda and Kondoh, 1999; Shimono et al., 1999). The peptides were coupled with keyhole limpet hemocyanin (KLH) and were used to immunize rabbits.

Immunoblotting Analysis

The sciatic nerves of the intact side and the proximal and distal stumps of the operated side at 9 days after the crush injury were homogenized in 500 ml of 1 mM $NaHCO_3$ buffer (pH 7.2) and centrifuged at 9,000 *g* for 15 min at 4°C. The supernatants were subjected to SDS-PAGE and immunoblotting analysis as described previously (Yamanaka et al., 1997), using a pAb to NDRG1 and peroxidase-conjugated goat anti-rabbit IgG (Jackson, West Grove, PA) diluted at 1:1,000 and 1:10,000, respectively.

TABLE 1. Other Primary Antibodies Used in Immunohistochemical Procedures

Antibody (clone)	Structure/ cell recognized	Source	Dilution	Species
MBP	Myelin	Chemicon	1:100	Rat
NF (NE14)	Axons	Boehringer	1:20	Mouse
S-100	Schwann cells	Bio Makor	1:1000	Mouse
BrdU (biotinylated)	Proliferating cells	Oncogene	Ready-to-use	Mouse
S-100	Schwann cells	Nichirei	1:10	Rabbit

Surgical Procedures

Adult male mice (C57BL6) weighing 20–25 g were used for all experiments. The left sciatic nerve was crushed for 30 s with jeweler's forceps at the mid-thigh level under pentobarbital anesthesia. After the surgery, kanamycin sulfate was sprayed over the entire surgical area and the wound was sutured. The intact contralateral side served as a control. Three mice were sacrificed on each of days 1, 2, 3, 7, 9, 14, and 21 after the operation.

The animals were anesthetized with ether, followed by intracardiac perfusions with 0.01 M phosphate-buffered saline (PBS) and then 4% paraformaldehyde in 0.1 M phosphate buffer (PB). The sciatic nerves were removed at a length of about 6 mm, and consisted of the proximal part (2-mm length), the crush injury site (1-mm length) and the distal part (3-mm length). The segments were postfixed with the same fixative for 3 h and immersed in 15% sucrose in 0.1M PB. They were then embedded in Embedding Matrix and immediately frozen with dry ice and isopentane. Longitudinal and transverse serial sections (10-μm thickness) were cut by using a cryostat microtome.

Immunohistochemistry

The immunohistochemical procedure used in the present study has been described elsewhere (Hirata et al., 2003). Briefly, cryostat sections were fixed again with 100% methanol for 10 min at −20°C and then washed with PBS. Nonspecific binding sites were blocked by preincubation with 1% bovine serum albumin (BSA) or 10% Block Ace (Yukijirushi, Sapporo, Japan) in PBS for 1 h at room temperature (RT). For NDRG1 immunohistochemistry, sections were first incubated with a pAb to NDRG1 diluted 1:100 in PBS overnight at RT and then with fluorescein isothiocya-

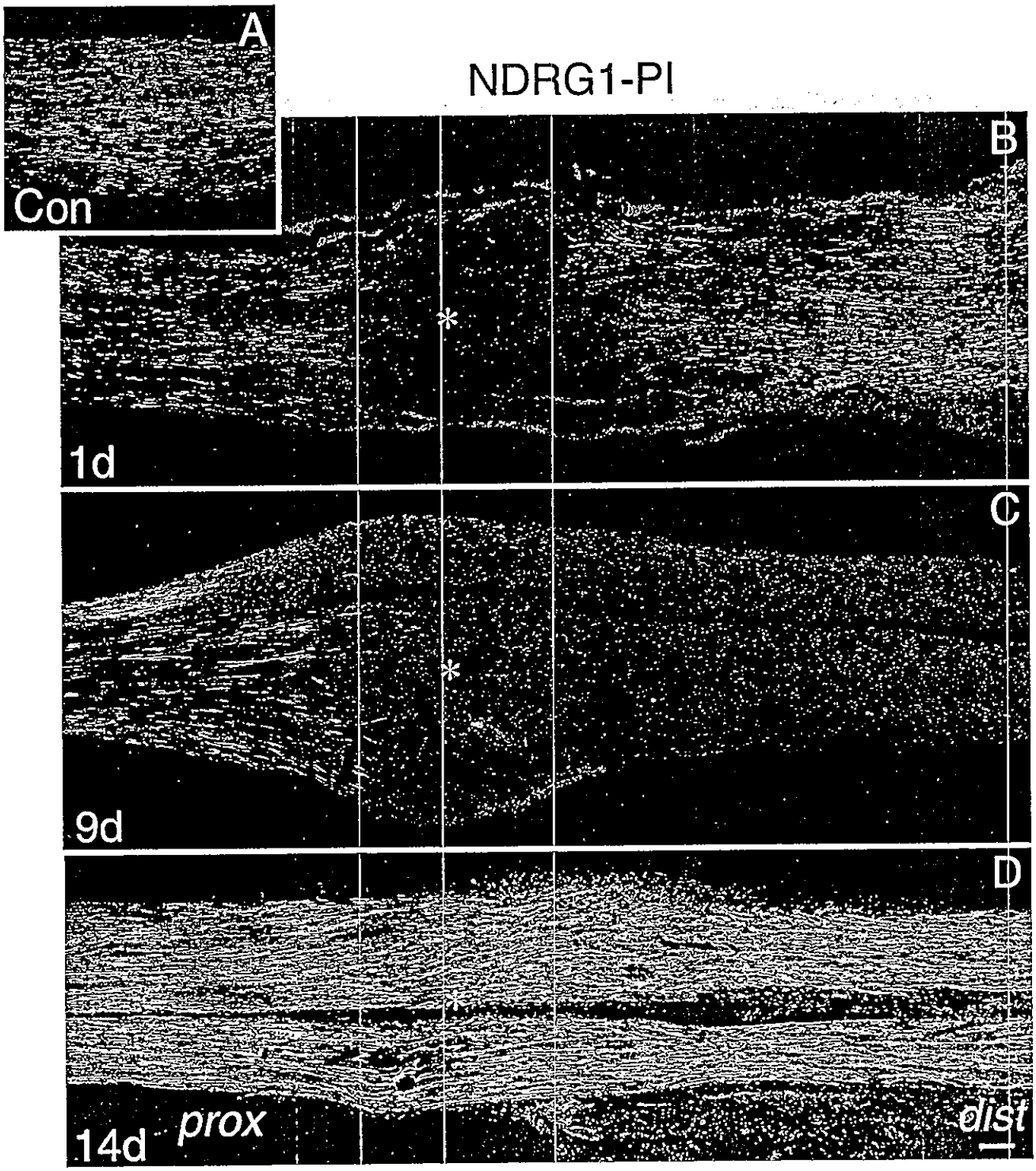

Fig. 1. Expression of NDRG1 (green) in longitudinal sections of intact sciatic nerve used as a control (A) and sciatic nerves at 1 day (B), 9 days (C), and 14 days (D) after crush injury. Moderate NDRG1-immunoreactive (-ir) structures seen in the intact nerve (A) remain in the distal stump at 1 day (B), but are hardly detected there at 9 days (C). The NDRG1-ir structures reappear with stronger immunoreactivity than that in the intact nerves at 14 days (D). Asterisks show the crush injury site. The distal and proximal stumps are indicated by dist and prox, respectively. Red indicates nuclei stained by PI. Scale bar = 50 μm

nate (FITC)-conjugated horse anti-rabbit IgG (Vector, Burlingame, CA) for 4 h at room temperature (RT). Control sections were processed identically and in parallel, except that they were incubated with PBS instead of the pAb to NDRG1. No stained cells were seen in these controls. To identify the nuclei of the cells, the

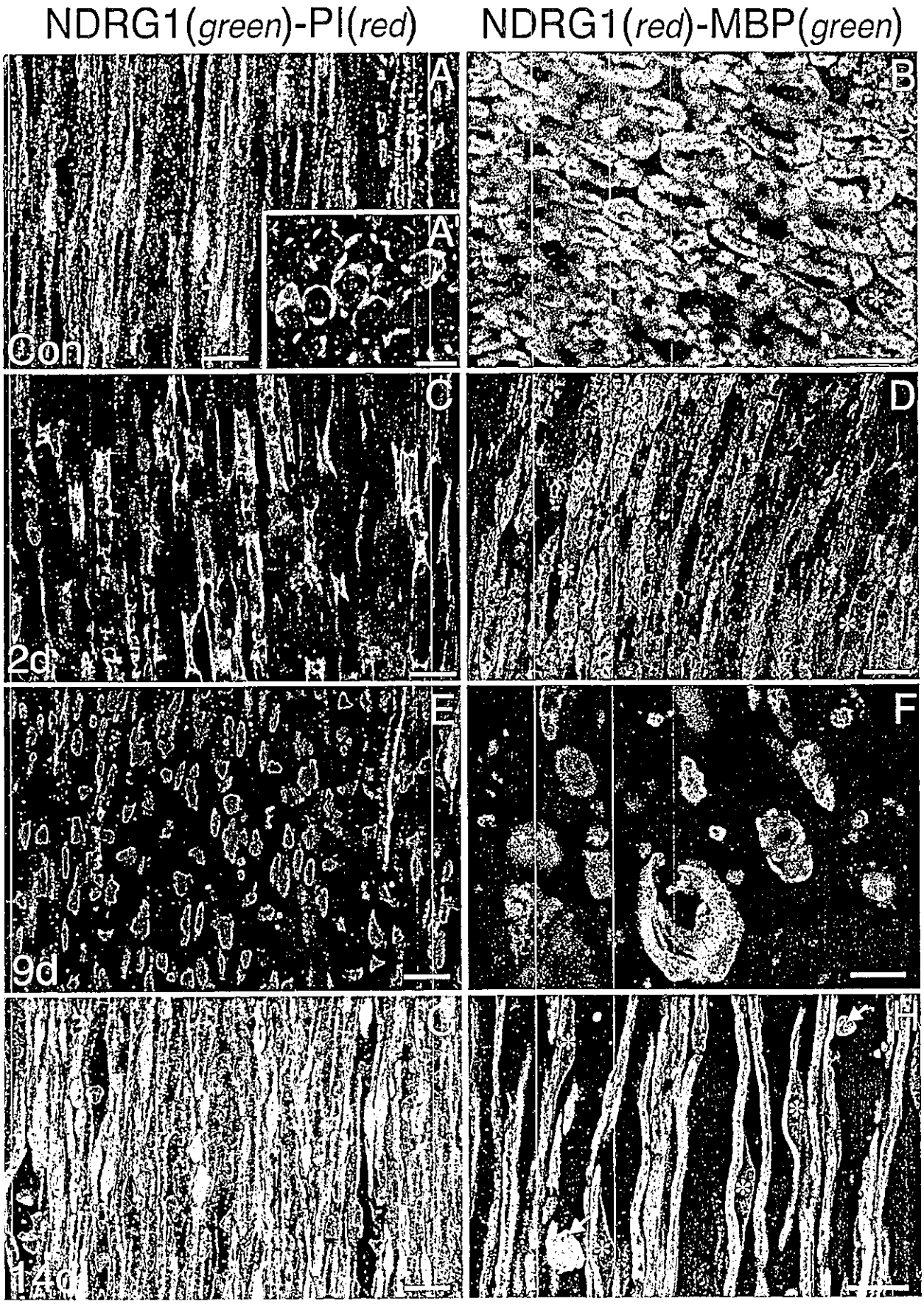
NDRG1(green)-PI(red)
NDRG1(red)-MBP(green)
A
A
B
0on
C
D
2d
E
F
9d
G
H
14d

Figure 2.

sections were counterstained with propidium iodide (PI) by using a Vectashield mounting medium containing PI (Vector).

To understand the time course of Wallerian degeneration and ensuing regeneration, double immunofluorescent labeling of NDRG1 with a myelin marker (Table 1) was performed. A mixture of a rabbit pAb to NDRG1 and a rat monoclonal antibody (mAb) to myelin basic protein (MBP) was used as the primary antibody. Then, a mixture of Texas red-conjugated donkey anti-rabbit IgG (Jackson) and FITC-conjugated donkey anti-rat IgG (Jackson) was used as the secondary antibody.

Furthermore, double immunofluorescent labeling of NDRG1 with axonal or SC markers (Table 1) was performed. A mixture of a rabbit pAb to NDRG1 and either a mouse mAb to 200-kDa neurofilament protein (NF) or to a mouse mAb to S-100 protein (S-100) was used as the primary antibody. Then, a mixture of FITC-conjugated horse anti-mouse IgG (Vector) and Texas red-conjugated donkey anti-rabbit IgG (Jackson) was used as the secondary antibody. No difference in morphology was noted in any of the immunolabeled structures between the single and double labeling.

To identify mitotic activity of SCs, double immunofluorescent labeling of bromodeoxyuridine (BrdU) and S-100 (Table 1) was performed. Mice were injected intraperitoneally with BrdU (Zymed, CA) (1 ml/100 g) 2 h or 2.5 h prior to being sacrificed. The nerve sections were incubated with a pAb to S-100 as a primary antibody and visualized by Texas red-conjugated donkey anti-rabbit IgG. For subsequent BrdU labeling, part of a BrdU staining kit (Oncogene Research, MA) was used; after treatment with HCl, the biotinylated mouse mAb to BrdU was used as primary antibody. The BrdU binding sites were visualized with streptavidin-FITC (Vector). Double immunofluorescent labeling of NDRG1 and BrdU was attempted, but was unsuccessful since the anti-NDRG1 staining was not compatible with the HCl treatment required for BrdU detection.

Confocal Laser Scanning Microscopy

The sections double-labeled with FITC and PI or FITC and Texas red were scanned with a confocal laser scanning imaging (CLSM) system (LSM-GB200, Olympus, Japan) using excitations at 488 nm (argon laser) for FITC and 568 nm (krypton laser) for PI or Texas red. Single optical sections for each fluorescence were taken separately (channel 1 and channel 2) to avoid any cross-talk and then superimposed. The images were taken using a ×10, ×20, ×40, or ×60 objective lens.

These experiments were reviewed by the Committee on Ethics for Animal Experiments of the Faculty of Medicine, Kyushu University and carried out according to the Guidelines for Animal Experiments of the University, and Law No. 105 and Notification No. 6 of the Japanese government.

RESULTS

In intact sciatic nerves, NDRG1 was expressed over the nerve (Fig. 1A). At 1 day after the crush injury, the expression showed no change except for its disappearance at the injury site (Fig. 1B). At 7–9 days after the crush injury, drastic depletion of the NDRG1 expression was seen at the injury site and the distal stump (Fig. 1C). The expression of NDRG1 then recovered at the injury site and the distal stump at 14 days after the crush injury, showing a slight increase in the immunoreactivity compared to that in the intact nerve (Fig. 1D). Higher magnification of longitudinal (Fig. 2A) and transverse (Fig. 2A′) sections of the intact nerve double-stained with PI nuclear staining showed that NDRG1 immunoreactivity was usually localized in the perinuclear cytoplasm of presumptive SCs of each fiber. Double immunofluorescent labeling with MBP revealed that MBP-immunoreactive (-ir) myelin sheath was usually surrounded by NDRG1-ir cytoplasm (Fig. 2B). At 2 days, cells in the distal stump transformed into cells containing various size of vacuoles, which are known to be characteristic for myelin-phagocytosing cells (Fig. 2C) and double labeling with MBP showed that MBP-ir degraded myelin structures were contained in the vacuoles of NDRG1-ir cells (Fig. 2D). At 7–9 days, NDRG1-ir cells were hardly detected in the injury site (Fig. 2E) and distal stumps (Fig. 2F), where the clearance of myelin debris was considerably progressed (Fig. 2F). At 2 weeks, numerous NDRG1-ir cells with a regular profile similar to that in intact nerves reappeared and the immunoreactivity was stronger than that in the intact nerve (Fig. 2G), and double labeling with MBP revealed that NDRG1-ir cells were in the process of myelinating (Fig. 2H).

Fig. 2. Pseudocolor images of double labeling of NDRG1 (green) with PI (red) (left panel: A,A′,C,E,G) and of double immunofluorescent labeling of NDRG1 (red) and MBP (green) (right panel: B,D,F,H) of intact nerves (A,A′,B), and of the injury site (E) and the distal stump (C,D,F–H) of crush-injured nerves. All pictures are from longitudinal sections, except for A′,B, which are from transverse sections. Asterisks (B,D,H) indicate sites of nuclei. A,A′,B: In intact nerves NDRG1 immunoreactivity is detectable in the perinuclear region of cytoplasm of the presumptive Schwann cells (green in A,A′). B: NDRG1-ir cells are myelinating cells, in which MBP-ir myelin sheath (green) are surrounded by a thin layer of NDRG1-ir cytoplasm (red). C,D: At 2 days, NDRG1-ir cells (green in C, red in D) have transformed into myelin-phagocytosing cells. D: The vacuoles of the cells seen in C are occupied by MBP-ir degraded myelin structures (green).E,F: At 9 days, no clearly stained NDRG1 -ir cells are seen both in the injury site (E) and the distal stump (F). E: Small number of NDRG1 cells seen at the boundary toward the proximal stump (upper). Note that only MBP-ir myelin debris can be seen (green in F). G,H: At 14 days, the NDRG1-ir cells reappear showing immunoreactivity stronger (G) than that in the intact nerve (A). H: NDRG1-ir cells are just forming a myelin sheath, judging from the prominent profiles of the perinuclear region (red) and thin MBP-ir myelin sheath (green). Note that strong NDRG1 immunoreactivity is seen not only in the perinuclear region also in the nuclear sites of some cells, suggesting translocation of the protein into nucleus. Arrows indicate the myelin debris. Scale bar = 10 μm.

To identify NDRG1-ir elements, double immunofluorescent labeling with NF, a neuronal marker, or S-100, an SC marker, was carried out. In the cross section of the intact nerve, the NDRG1-ir structure could clearly be distinguished from the NF-ir axons, since the former was localized in the peripheral region of a nerve fiber so that it appeared as a ring-like structure and the latter was in the central part (Fig. 3A). In contrast, the immunoreactive sites of NDRG1 were almost identical with those of S-100 in the intact nerve, suggesting that the NDRG1 was contained only in SCs (Fig. 3B,C). NDRG1 continued to be expressed in S-100-ir SCs, which had the characteristics of myelin-phagocytosing cells at 2 days after the crush injury (Fig.3D,E). At the next stage (7–9 days), the expression of NDRG1 was markedly reduced, whereas the S-100-ir SCs were further transformed to cells with irregular contour (Fig. 3F,G). At the ensuing stage (2 weeks), NDRG1 was reexpressed in S-100-ir SCs, which now showed a regular structure similar to that in the intact nerves.

In the process of nerve regeneration, SCs are known to proliferate following transformation into myelin-phagocytosing cells, and then acquire the immature phenotype to promote axonal regrowth (for review, see Hirata and Kawabuchi, 2002). Double immunofluorescent labeling of BrdU and S-100 was carried out to identify the mitotic activity of SCs. In intact nerves, no cells with BrdU-labeled nuclei were found. At 2 days, only a few S-100-ir SCs with BrdU-labeled nuclei appeared, although presumptive macrophages with BrdU-labeled nuclei were often observed in the perineurium or the epineurium. At 7–9 days (Fig. 4A,C), when the transient depletion of NDRG1 expression occurred, numerous SCs with BrdU-labeled nuclei were detected and distributed throughout the injury site and the distal stump. At 2 weeks, the number of cells with BrdU-labeled nuclei markedly decreased. Thus, the results suggested an inverse relationship between the proliferative activity and NDRG1 expression of SCs. The specificity of BrdU labeling was confirmed in the small intestine (Fig. 4B), where the cells with BrdU-labeled nuclei were specifically distributed in the base of the crypts, known to be the proliferative zone (Potten et al., 1997).

Immunoblotting analysis of sciatic nerves at 9 days after the crush injury revealed that the pAb to NDRG1 labeled a polypeptide band of 43 kDa in the intact nerve (Fig. 5B, lane 1) and the proximal stumps (Fig. 5B, lane 2) but not the distal stumps (Fig. 5B, lane 3) of the crushed nerve. This finding not only confirmed the specificity of the antibody but also indicated preferential depletion of NDRG1 molecules in the injured nerves at this time point. No specific labeling was observed in the control probed with normal rabbit sera.

DISCUSSION

In the present study, immunofluorescent histochemistry and Western blotting analysis using NDRG1 antibodies demonstrated that NDRG1 was expressed in intact mouse sciatic nerve. Double immunofluorescent labeling with an SC marker (S-100) or an axonal marker (NF) showed that NDRG1 was localized in the cytoplasm of SCs, but not in the axons. These findings agree with those of human peripheral nerves analyzed by Northern blotting and RT-PCR (Kalaydjieva et al., 2000) and an immunoenzyme-histochemical technique (Lachat et al., 2002).

Double immunofluorescent labeling of NDRG1 and MBP revealed that NDRG1 was expressed in the cytoplasm of myelinating SCs in intact nerves. Crushed nerves showed little alteration of NDRG1 expression when the myelinating SCs transformed into myelin-phagocytosing cells in the early stage of myelin degradation (Stoll et al., 1989; Hirata et al., 1999). This finding implies that the expression of this protein in SCs is not influenced by either the loss of axonal contact or the transformation of SCs into myelin-phagocytosing cells. Thus, NDRG1 expression does not appear to be regulated during Wallerian degeneration. In contrast, the expression of this protein changed markedly during subsequent process. Both immunohistochemistry and Western blotting analysis demonstrated that NDRG1 expression was dramatically depleted at 7–9 days after the operation, when the myelin removal was considerably progressed. NDRG1 was then reexpressed with more immunoreactivity than that of the intact nerves during remyelination. Thus, our study suggests that NDRG1 may be regulated in the regeneration process of injured nerves.

It is well known that, after taking part in the early stage of myelin removal, SCs proliferate to acquire the immature phenotype and prepare the environments through which regenerating axons grow (for review, see Fawcett and Keynes, 1990; Jessen and Mirsky, 1999; Hirata and Kawabuchi, 2002). In the present study, frequent occurrences of BrdU-labeled SCs were seen at 7–9 days after the crush injury, the timing of which is largely consistent with the occurrence of SC mitosis observed by electron microscopy (O'Daly and Imaeda, 1967). It is noteworthy that the drastic depletion of NDRG1 occurred simultaneously during this period. NDRG1 was reported to be developmentally regulated in embryonic tissues and to be augmented concomitantly with the occurrence of terminal differentiation (Shimono et al., 1999). Direct subtraction of whole mouse embryo cDNAs between the wild type and an N-myc mutant (Shimono et al., 1999) revealed that the NDRG1 gene was repressed by N-myc, a member of the myc family that encodes nuclear phosphoproteins and is believed to play a role in the control of cellular proliferation and differentiation (Melhem et al., 1992). Several lines of in vitro evidence have suggested a role for NDRG1 in cells undergoing terminal differentiation. For example, the NDRG1 gene was upregulated during the differentiation of colon carcinoma cell lines cultured in low glucose medium (van Belzen et al., 1997) and during in vitro forskolin-induced differentiation of a model of the human trophoblast, the chorio-

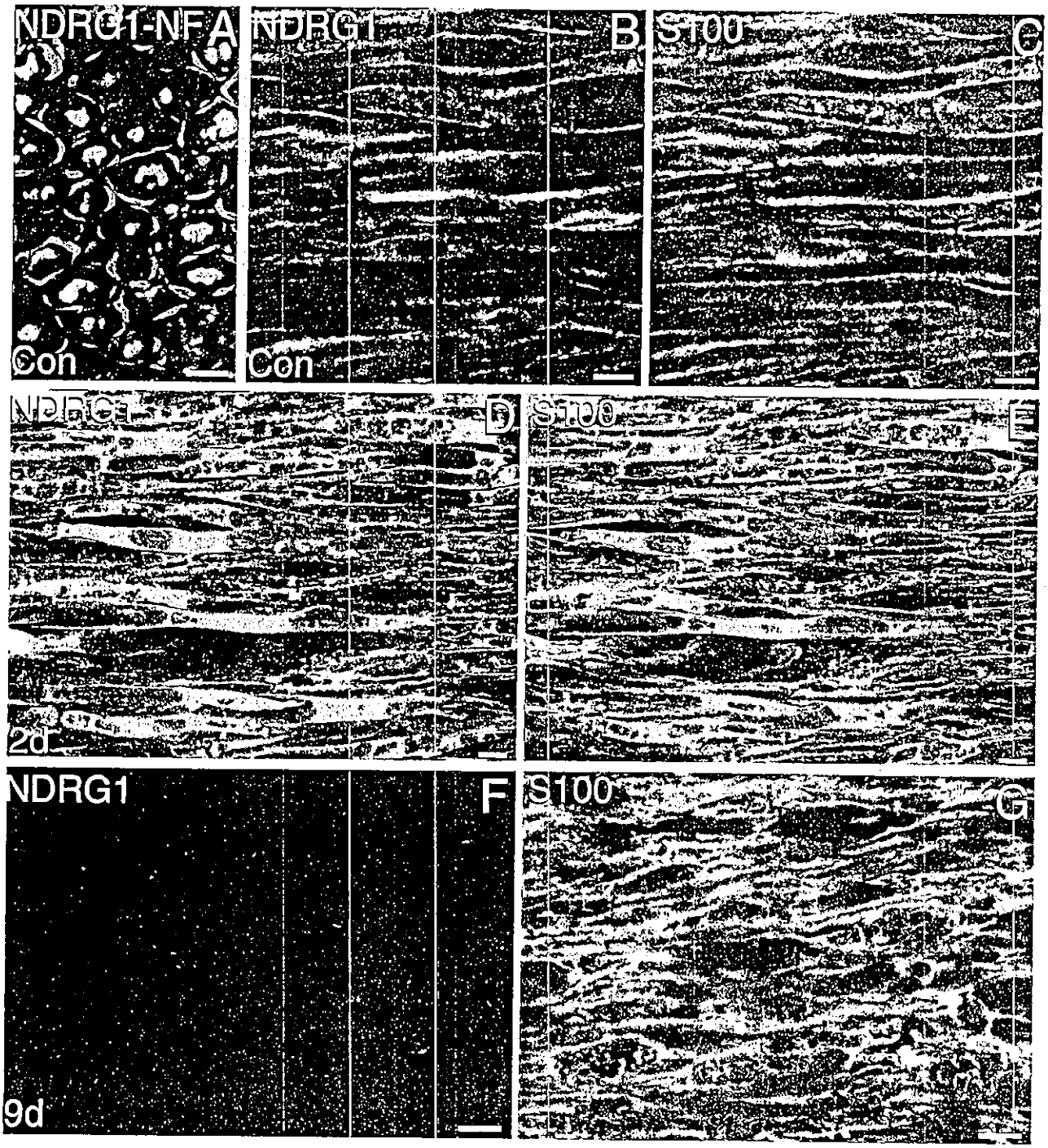

Fig. 3. Gray scale image of double immunofluorescent labeling of NDRG1 and NF in a transverse section of an intact nerve (A) and grayscale images of NDRG1 (B,D,F) and S-100 (C,E,G), in which each of the images is separately displayed, in longitudinal sections of an intact nerve (B,C) and the distal stumps of nerves at 2 days (D,E) and 9 days (F,G) after crush injury. A–C: In intact nerves the distribution of NDRG1 (gray in A) and NF immunoreactivity (white in A) is clearly distinguished, since the former is seen in the periphery (cf. Fig. 2A') of the round profile of each fiber and the latter is in the center. On the other hand, the NDRG1-ir sites (B) are almost identical to the S-100-ir sites (C), suggesting that NDRG1 is localized in the cytoplasm of Schwann cells, but not in axons. D–G: At 2 days, the expression of NDRG1 (D) is maintained in the S-100-ir Schwann cells which have transformed into myelin-phagocytosing cells (E), but at 9 days, the expression (F) is hardly detected in S-100-ir Schwann cells with a irregular profile (G). Scale bar = 10 μm.

carcinoma BeWo (Xu et al., 1999). The expression of NDRG1 protein was upregulated in the macrophage differentiation of leukemic U937 cells induced by treatment with 1,25-$(OH)_2$ vitamin D_3 or retinoic acid (Piquemal et al., 1999). Furthermore, stable transfection of a colon cancer cell line with NDRG1 cDNA

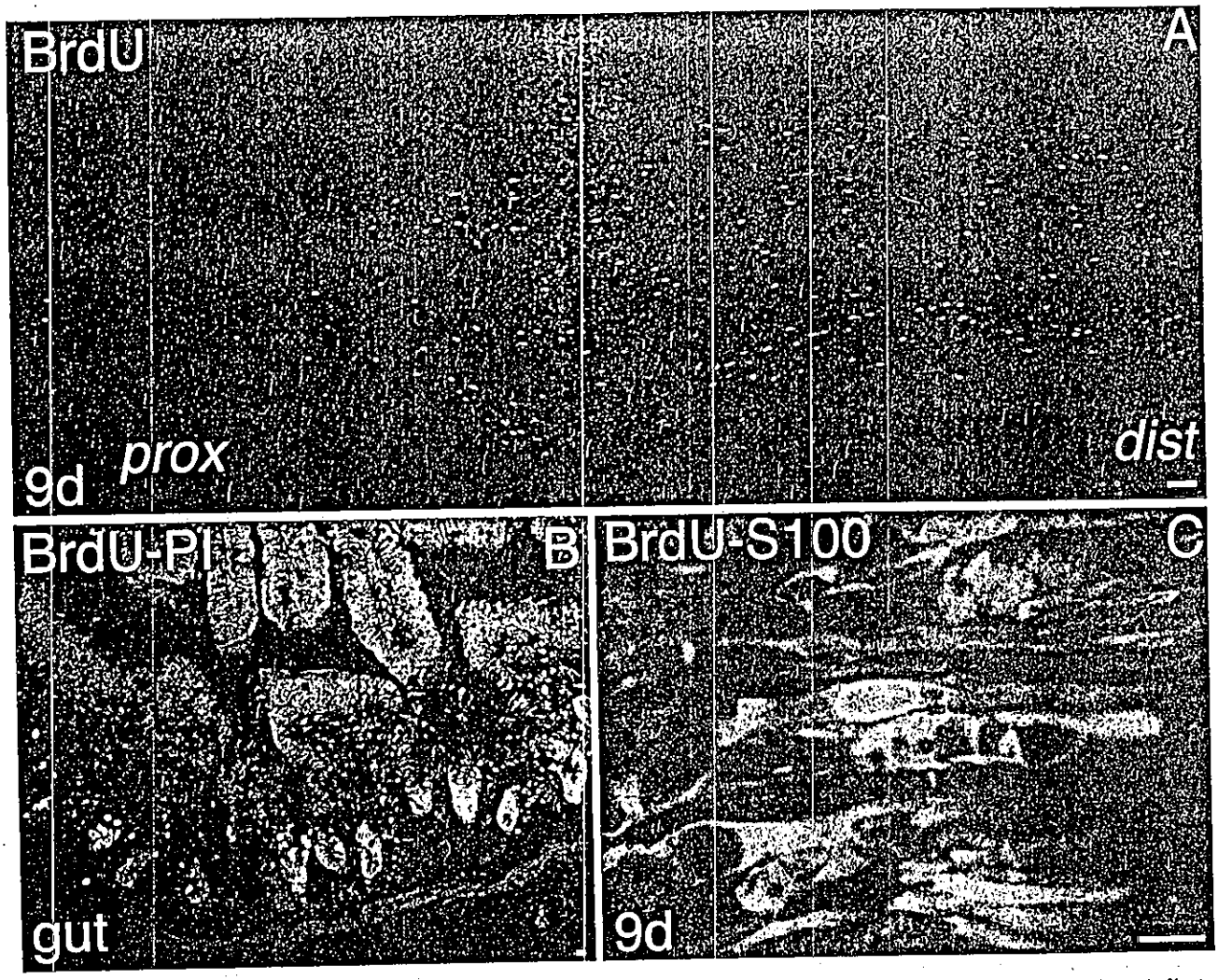

Fig. 4. BrdU immunofluorescent labeling of the nerve at 9 days after crush injury (A,C) and normal mouse jejunum as a positive control (B). A: In a longitudinal section of the nerve BrdU-labeled cells (white) are only distributed in the distal stump and the injury site, corresponding to the area where a marked depletion of NDRG1 is seen (cf. Fig. 1C). B: In a transverse section of the gut BrdU-labeled epithelial cells (white) are only located in the base of the crypts, to which cell proliferation is known to be restricted. Gray indicates PI-stained structures. C: In a higher-magnification image of the distal stump the double immunofluorescent labeling of BrdU (white) and S-100 (gray) shows that the nucleus of an S-100-ir cell is positive for BrdU, suggesting the mitotic activity of Schwann cells. Scale bars = 50 μm in A; 10 μm in B,C.

induced morphological and phenotypic changes indicative of differentiation, suggesting its possible role as a metastatic suppresser gene (Guan et al., 2000). Kurdistani et al. (1998) demonstrated that this gene was a p53-responsive gene with anti-proliferative properties, and that it was regulated in a cell cycle-dependent manner. These in vitro findings were supported by in vivo observations using in situ hybridization or immunohistochemical techniques showing that NDRG1 was expressed in the terminally differentiated cells in some organs, in which cell renewal is detectable under physiological conditions, such as colon epithelial cells (van Belzen et al., 1997), and skin keratinocytes (Gomez-Casero et al., 2001). Our immunohistochemical study on injured sciatic nerves revealed that the expression of NDRG1 was depleted in de-differentiated SCs and recovered in re-differentiated SCs with more immunoreactivity than that in the SCs of intact nerves. Thus, our findings suggest a role for NDRG1 in the terminal differentiation, including myelination, of SCs in nerve regeneration.

In a patient with HMSNL in whom a premature termination codon of the NDRG1 gene was found, one of the main neuropathological features of the disease was SC dysfunction, such as hypomyelination and demyelination/remyelination, failure of compaction of the innermost myelin lamellae, and poor hypertrophic response to the demyelination process (Kalaydjieva et al., 2000). It seems reasonable to surmise that this may be a direct effect of NDRG1 dysfunction, because this protein resides in SCs, especially myelinating ones. Kalaydjieva et al. (2000) inferred that the putative phosphopantetheine-binding domain present in NDRG1 protein (Kokame et al., 1996) may possibly be involved

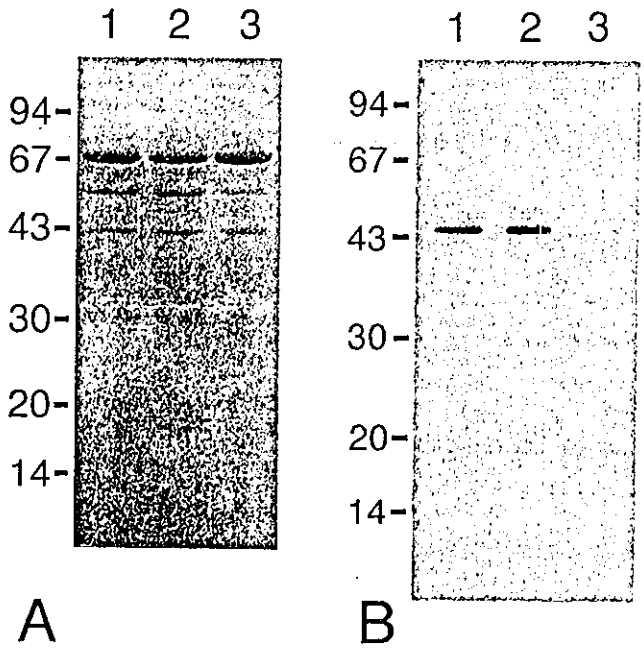

Fig. 5. Immunoblotting analysis of mouse sciatic nerves with a rabbit pAb to NDRG1. The samples were obtained at 9 days after crush injury. The amido black-stained sodium dodecyl sulfate-polyacrylamide gel electrophoresis (SDS-PAGE) profiles (A) and immunoblotted samples (B) from the intact side (lane 1), and the proximal stump (lane 2) and distal stump (lane 3) of the operated side are shown. The molecular weight markers (kDa) are indicated on the left.

in the lipid biosynthetic pathways operating in the myelinating SCs. On the other hand, Lachat et al. (2002) pointed out that the decompaction of the myelin sheath in the disease may be due to dysfunction of the adherens junctions in Schmidt-Lanterman incisures (Colman et al., 2001) based on their immunohistochemical findings that in all the examined epithelial cell types membrane labeling was observed predominantly adjacent to adherens junctions. Another prominent neuropathological feature of HMSNL is axonal involvement, such as early, severe, and progressive axonal loss (Kalaydjieva et al., 2000). Kalaydjieva et al. (2000) interpreted that NDRG1 may also have a role in the PNS, possibly in the SC signaling necessary for axonal survival, from their assumption that NDRG1 is possibly involved in SC differentiation, since differentiating SCs are an important source of signals for the development of nerves, in addition to controlling neuronal survival (Jessen and Mirsky, 1999). Our findings for NDRG1 expression in the process of nerve regeneration appear to support their hypothesis. However, further study is needed to clarify the exact role of NDRG1 in nerve development, since recent studies have stressed that the developmental process of the nerves is not always identical to the regenerative process, especially regarding the molecular mechanisms regulating SC proliferation (Kim et al., 2000; Atanasoski et al., 2001).

Besides the involvement of the NDRG1 in cell differentiation, this gene has been reported to be modulated under conditions of cellular stress that were caused by homocysteine (Kokame et al., 1996; Agarwala et al., 2000), forskolin (Xu et al., 1999), androgen (Segawa et al., 2002), nickel exposure (Salnikow et al., 2000), and hypoxia (Salnikow et al., 2000; Lachat et al., 2002). Our previous studies demonstrated that two different kinds of heat shock proteins (HSPs), 32 kDa-heat shock protein (Hirata et al., 2000) and 27 kDa-heat shock protein (Hirata et al., 2003) were differentially induced in different phases of SCs after axotomy, since the former was induced in SCs that transformed into myelin-phagocytosing cells immediately after the injury, while the latter was induced in SCs in the next phase that formed the SC column for axonal guidance. In the present study, NDRG1 was reexpressed during remyelination with more immunoreactivity than the normal level, suggesting its involvement in myelination, which is the last phase of SC transformation. No previous investigators have reported that the NDRG1 belongs to the HSPs. However, it is likely that, in addition to HSP32 and HSP27, this protein could be acting as a molecular base, explaining the inherent ability of SCs to not only protect themselves from abnormal environments but also participate actively in the repair process, although it may play a role in maintaining tissue homeostasis in intact nerves.

ACKNOWLEDGMENTS

The authors thank Mr. Yasuhiro Hirakawa and Mr. Takaaki Kanemaru (Morphology Core, Graduate School of Medical Sciences, Kyushu University) for their help in preparing the photomicrographs, and Mr. Naoya Inakura for his expert technical assistance.

REFERENCES

Agarwala KL, Kokame K, Kato H, Miyata T. 2000. Phosphorylation of RTP, an ER stress-responsive cytoplasmic protein. Biochem Biophys Res Commun 272:641–647.

Atanasoski S, Shumas S, Dickson C, Scherer SS, Suter U. 2001. Differential cyclin D1 requirements of proliferating Schwann cells during development and after injury. Mol Cell Neurosci 18:581–592.

Bandyopadhyay S, Pai SK, Gross SC, Hirota S, Hosobe S, Miura K, Saito K. Commes T, Hayashi S, Watabe M, Watabe K. 2003. The Drg-1 gene suppresses tumor metastasis in prostate cancer. Cancer Res 63:1731–1736.

Colman DR, Pedraza L, Yoshida M. 2001. Concepts in myelin sheath evolution. In: Jessen KR, Richerdson WD, editors. Glial cell development. 2nd ed. Oxford: Oxford University Press. p 161–176.

Fawcett JW, Keynes RJ. 1990. Peripheral nerve regeneration. Annu Rev Neurosci 13:43–60.

Gomez-Casero E, Navarro M, Rodriguez-Puebla ML, Larcher F, Paramio JM, Conti CJ, Jorcano JL. 2001. Regulation of the differentiation-related gene Drg-1 during mouse skin carcinogenesis. Mol Carcinogen 32:100–109.

Guan RJ, Ford HL, Fu Y, Li Y, Shaw LM. Pardee AB. 2000. Drg-1 as a differentiation-related, putative metastatic suppressor gene in human colon cancer. Cancer Res 60:749–755.

Hirata K, Kawabuchi M, 2002. Myelin phagocytosis by macrophages and nonmacrophages during Wallerian degeneration. Microsc Res Tech 57:541–547.

Hirata K, Mitoma H, Ueno N, He J, Kawabuchi M. 1999. Differential response of macrophage subpopulations to myelin degradation in the injured rat sciatic nerve. J Neurocytol 28:685–695.

Hirata K, He J, Kuraoka A, Omata Y, Hirata M, Shariful Islam ATM, Noguchi M, Kawabuchi M. 2000. Heme oxygenase 1 (HSP-32) is induced in myelin-phagocytosing Schwann cells of injured sciatic nerves in the rat. Eur J Neurosci 12:4147–4152.

Hirata K, He J, Hirakawa Y, Liu W, Wang S, Kawabuchi M. 2003. HSP27 is markedly induced in Schwann cell columns and the associated regenerating axons. Glia 42:1–11.

Jessen KR, Mirsky R. 1999. Schwann cells and their precursors emerge as major regulators of nerve development. Trends Neurosci 22:402–410.

Kalaydjieva L, Gresham D, Gooding R, Heather L, Baas F, de Jonge R, Blechschmidt K, Angelicheva D, Chandler D, Worsley P, Rosenthal A, King RH, Thomas PK. 2000. N-myc downstream-regulated gene 1 is mutated in hereditary motor and sensory neuropathy-Lom. Am J Hum Genet 67:47–58.

Kim HA, Pomeroy SL, Whoriskey W, Pawlitzky I, Benowitz LI, Sicinski P, Stiles CD, Roberts TM. 2000. A developmentally regulated switch directs regenerative growth of Schwann cells through cyclin D1. Neuron 26:405–416.

Kokame K, Kato H, Miyata T. 1996. Homocysteine-respondent genes in vascular endothelial cells identified by differential display analysis. GRP78/BiP and novel genes. J Biol Chem 271:29659–29665.

Krauter-Canham R, Bronner R, Evrard JL, Hahne G, Friedt W, Steinmetz A. 1997. A transmitting tissue- and pollen-expressed protein from sunflower with sequence similarity to the human RTP protein. Plant Sci 129:191–202.

Kuidistani SK, Arizti P, Reimer CL, Sugrue MM, Aaronson SA, Lee SW. 1998. Inhibition of tumor cell growth by RTP/rit42 and its responsiveness to p53 and DNA damage. Cancer Res 58:4439–4444.

Lachat P, Shaw P, Gebhard S, van Belzen N, Chaubert P, Bosman FT. 2002. Expression of NDRG1, a differentiation-related gene, in human tissues. Histochem Cell Biol 118:399–408.

Lin TM, Chang C. 1997. Cloning and characterization of TDD5, an androgen target gene that is differentially repressed by testosterone and dihydrotestosterone. Proc Natl Acad Sci USA 94:4988–4993.

Melhem MF, Meisler AI, Finley GG, Bryce WH, Jones MO, Tribby II, Pipas JM, Koski RA. 1992. Distribution of cells expressing myc proteins in human colorectal epithelium, polyps, and malignant tumors. Cancer Res 52:5853–64.

Nishie A, Masuda K, Otsubo M, Migita T, Tsuneyoshi M, Kohno K, Shuin T, Naito S, Ono M, Kuwano M. 2001. High expression of the Cap43 gene in infiltrating macrophages of human renal cell carcinomas. Clin Cancer Res 7:2145–2151.

O'Daly JA, Imaeda T. 1967. Electron microscopic study of Wallerian degeneration in cutaneous nerve caused by mechanical injury. Lab Invest 17:744–766.

Okuda T, Kondoh H. 1999. Identification of new genes ndr2 and ndr3 which are related to Ndr1/RTP/Drg1 but show distinct tissue specificity and response to N-myc. Biochem Biophys Res Commun 266:208–215.

Piquemal D, Joulia D, Balaguer P, Basset A, Marti J, Commes T. 1999. Differential expression of the RTP/Drg1/Ndr1 gene product in proliferating and growth arrested cells. Biochim Biophys Acta 1450:364–373.

Potten CS, Booth C, Pritchard DM. 1997. The intestinal epithelial stem cell: the mucosal governor. Int J Exp Pathol 78:219–243.

Qu X, Zhai Y, Wei H, Zhang C, Xing G, Yu Y, He F. 2002. Characterization and expression of three novel differentiation-related genes belong to the human NDRG gene family. Mol Cell Biochem 229:35–44.

Salnikow K, Blagosklonny MV, Ryan H, Johnson R, Costa M. 2000. Carcinogenic nickel induces genes involved with hypoxic stress. Cancer Res 60:38–41.

Sato N, Kokame K, Shimokado K, Kato H, Miyata T. 1998. Changes of gene expression by lysophosphatidylcholine in vascular endothelial cells: 12 up-regulated distinct genes including 5 cell growth-related, 3 thrombosis-related, and 4 others. J Biochem 123:1119–26.

Segawa T, Nau ME, Xu LL, Chilukuri RN, Makarem M, Zhang W, Petrovics G, Sesterhenn IA , McLeod DG, Moul JW, Vahey M, Srivastava S. 2002. Androgen-induced expression of endoplasmic reticulum (ER) stress response genes in prostate cancer cells. Oncogene 21:8749–8758.

Shaw E, McCue LA, Lawrence CE, Dordick JS. 2002. Identification of a novel class in the alpha/beta hydrolase fold superfamily: the N-myc differentiation-related proteins. Proteins 47:163–168.

Shimono A, Okuda T, Kondoh H. 1999. N-myc-dependent repression of ndr1, a gene identified by direct subtraction of whole mouse embryo cDNAs between wild type and N-myc mutant. Mech Dev 83:39–52.

Stoll G, Griffin JW, Li CY, Trapp BD. 1989. Wallerian degeneration in the peripheral nervous system: participation of both Schwann cells and macrophages in myelin degradation. J Neurocytol 18:671–683.

Ulrix W, Swinnen JV, Heyns W, Verhoeven G. 1999. The differentiation-related gene 1, Drg1, is markedly upregulated by androgens in LNCaP prostatic adenocarcinoma cells. FEBS Lett 455:23–26.

van Belzen N, Dinjens WN, Diesveld MP, Groen NA, van der Made AC, Nozawa Y, Vlietstra R, Trapman J, Bosman FT. 1997. A novel gene which is up-regulated during colon epithelial cell differentiation and down-regulated in colorectal neoplasms. Lab Invest 77:85–92.

Xu B, Lin L, Rote NS. 1999. Identification of a stress-induced protein during human trophoblast differentiation by differential display analysis. Biol Reprod 61:681–686.

Yamanaka I, Kuraoka A, Inai T, Ishibashi T, Shibata Y. 1997. Changes in the phosphorylation states of connexin43 in myoepithelial cells of lactating rat mammary glands. Eur J Cell Biol 72:166–173

Zhou D, Salnikow K, Costa M. 1998. Cap43, a novel gene specifically induced by Ni2+ compounds. Cancer Res 58:2182–2189.